Induced seismicity during to the construction of the Gotthard base tunnel, Switzerland

Stephan Husen, Swiss Seismological Service, ETH Zurich

in collaboration with

E. Kissling (ETHZ), A. von Deschwanden (ETHZ), H. Hagedorn (Amberg Engineering), M. Rehbock-Sander (Amberg Engineering), T. Eppler (Amberg Engineering), S. Metzger (ETHZ), ELAB Team (ETHZ), and AG Mikrobeben working group.

Schweizerischer Erdbebendienst
Swiss Seismological Service

Gotthard base tunnel:

Total length: 57 km

Two parallel single track tubes with a diameter of 9.2 m.

Three intermediate access points for construction.

Access point of Faido will serve as multi-function section (MFS) for maintenance and rescue operations.

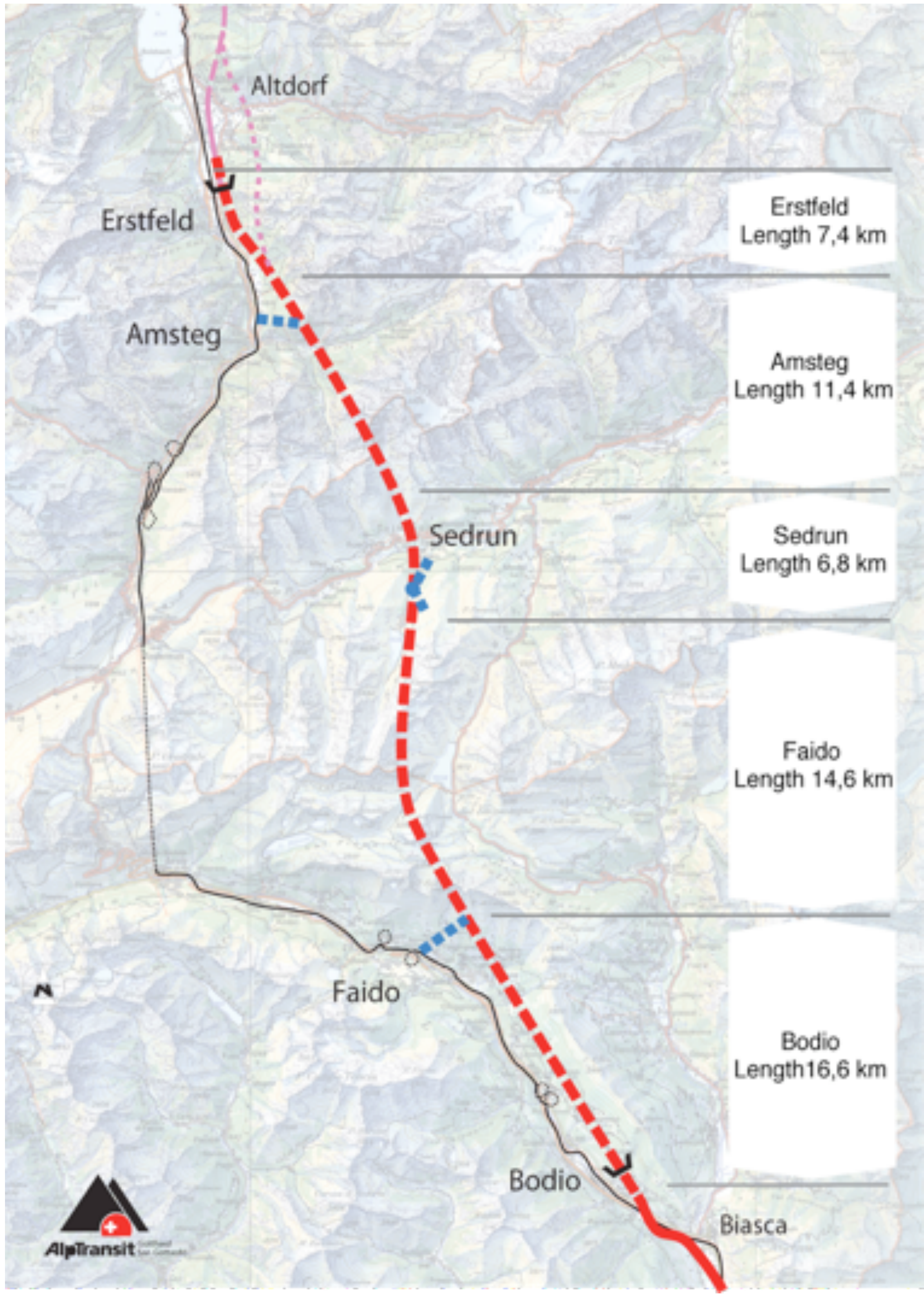

Gotthard base tunnel:

Total length: 57 km

Two parallel single track tubes with a diameter of 9.2 m.

Three intermediate access points for construction.

Access point of Faido will serve as multi-function section (MFS) for maintenance and rescue operations.

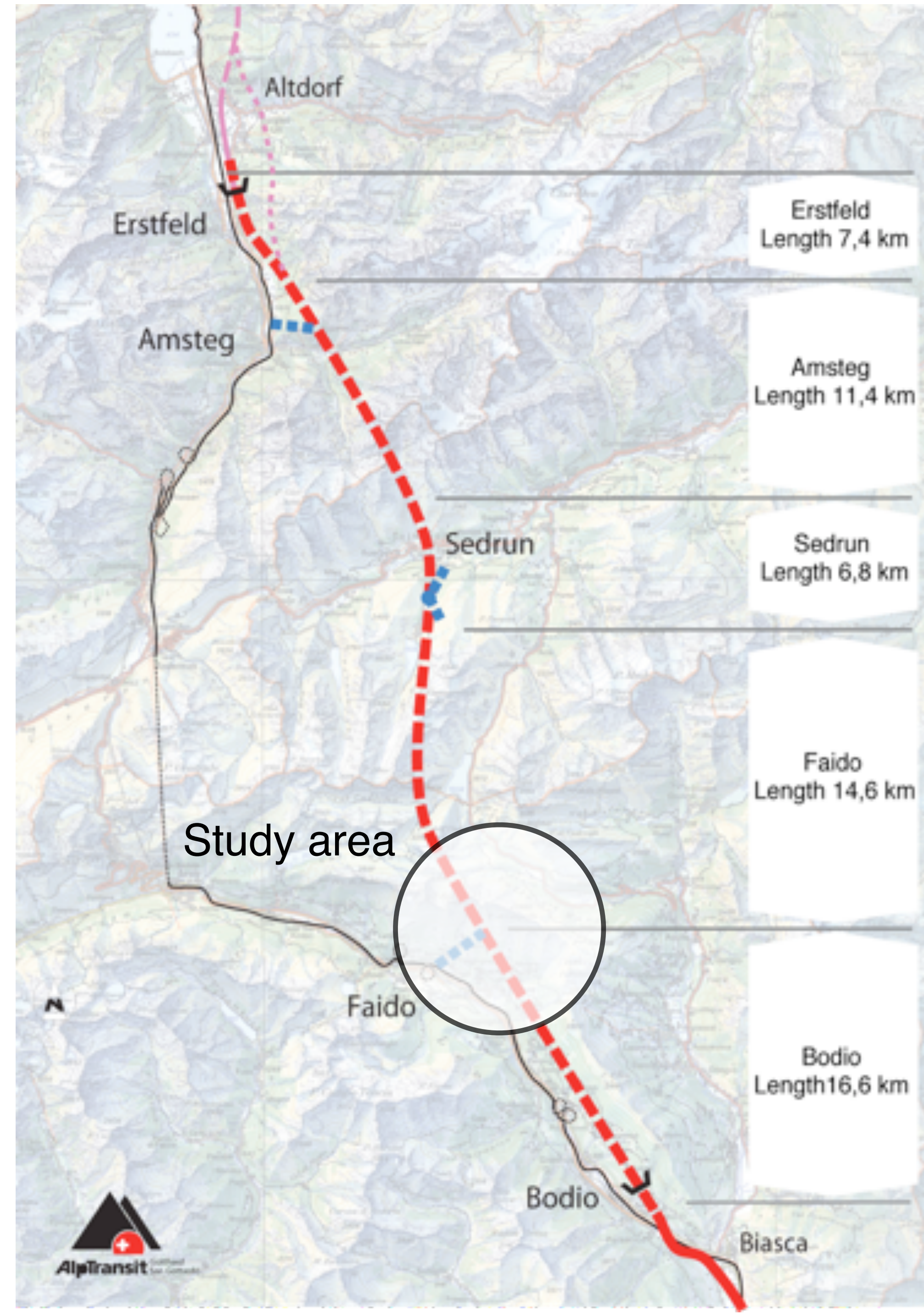

Main geologic units along Gotthard base tunnel:

MFS Faido is located in the Penninic gneisses.

Average overburden is ~1500 m.

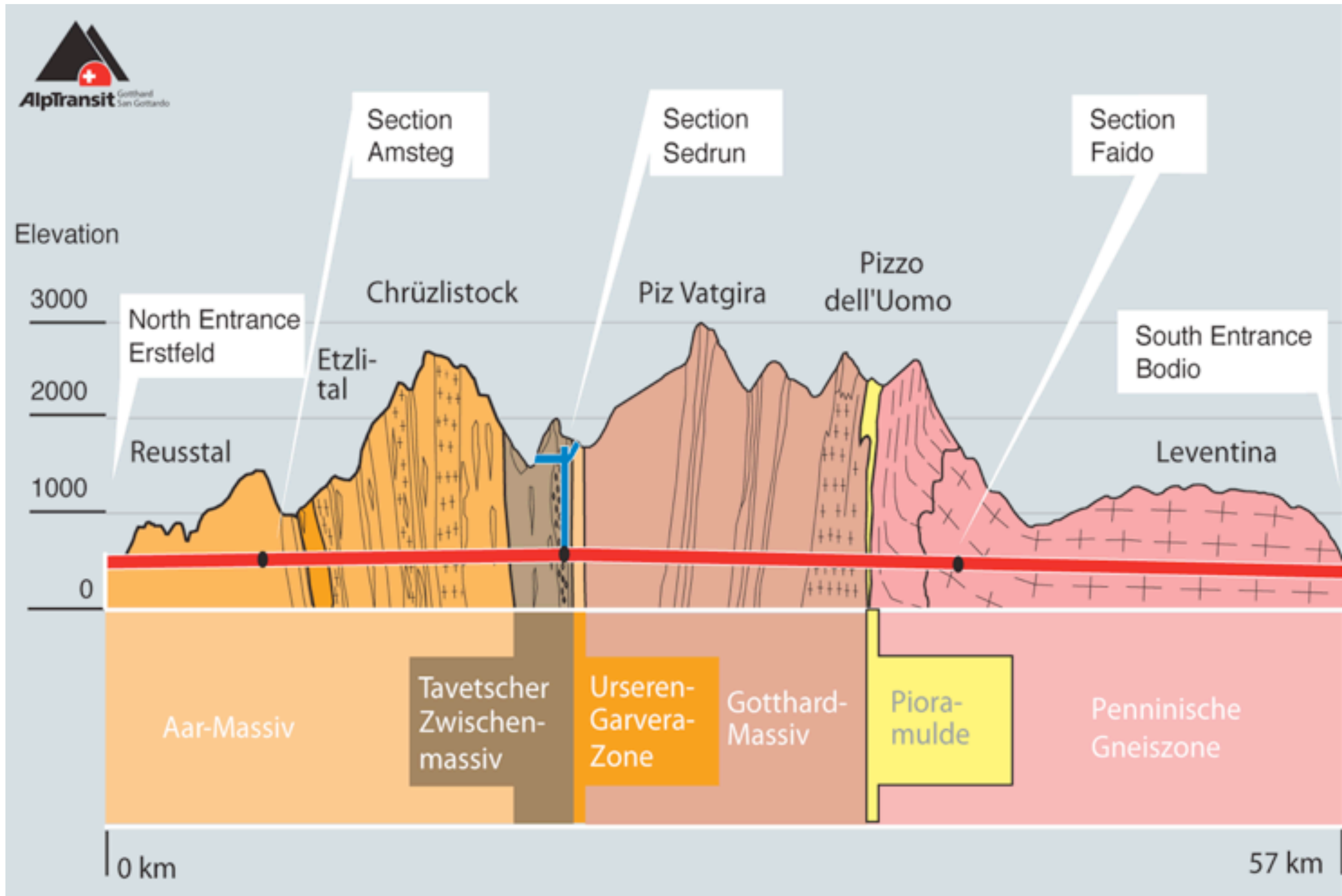

Geology within MFS Faido

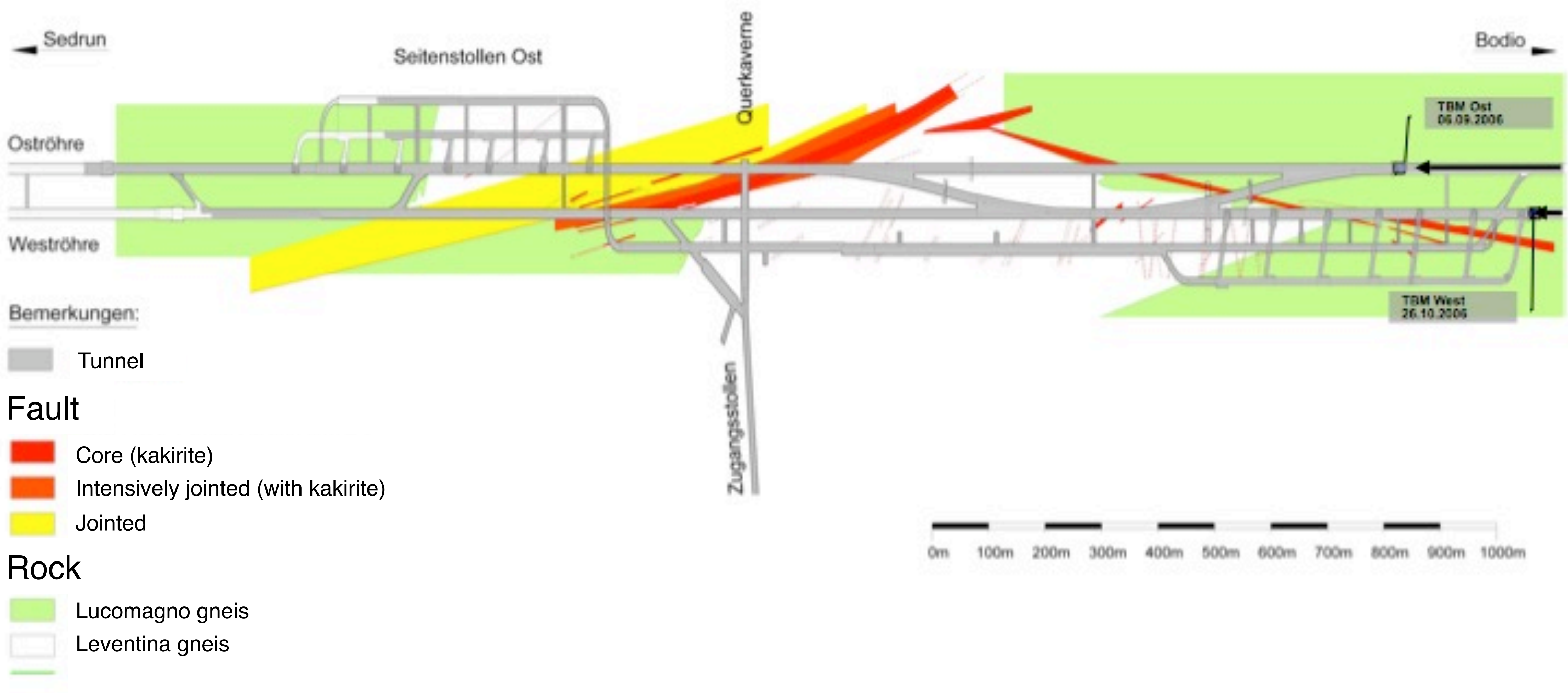

Geology within MFS Faido

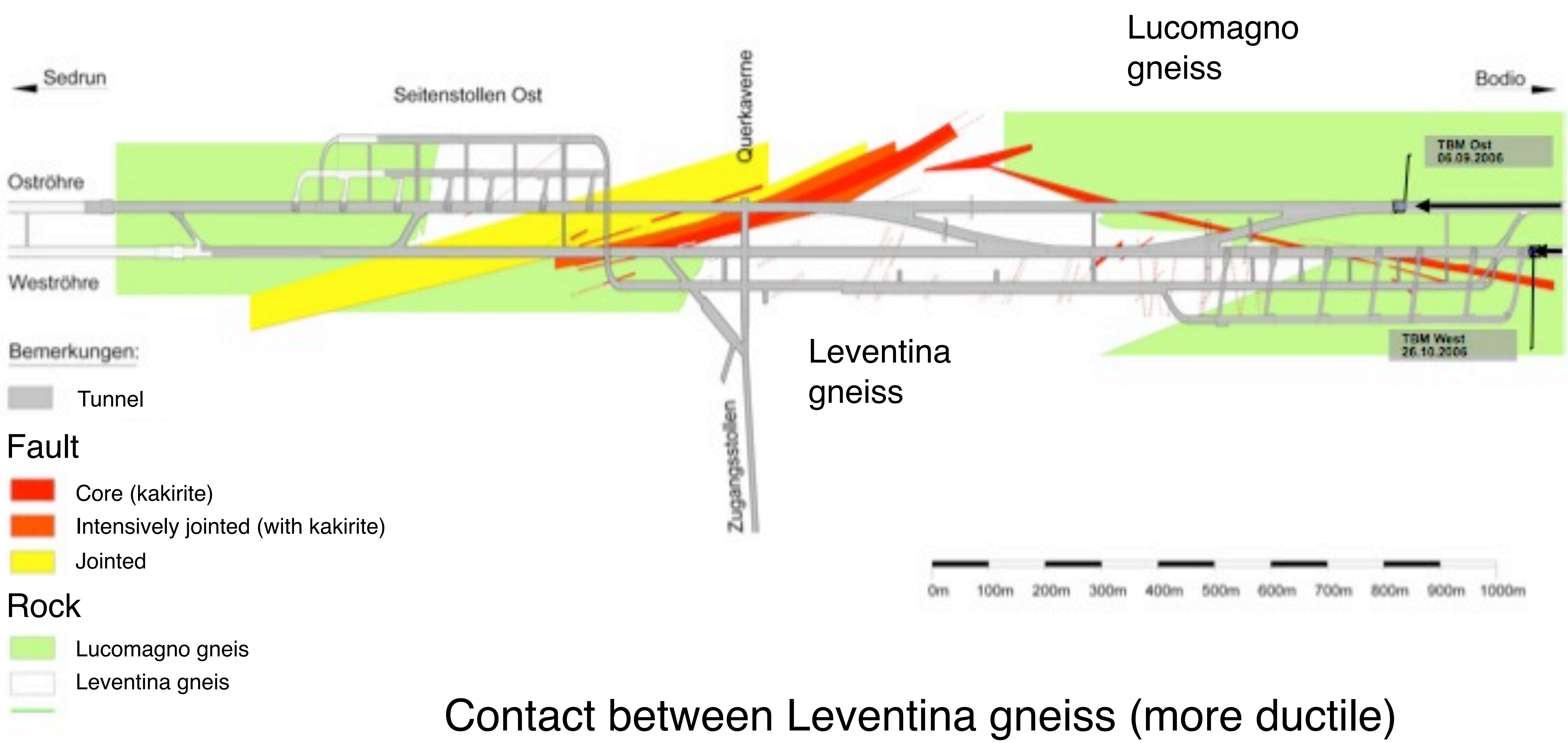

Contact between Leventina gneiss (more ductile) and Lucomagno gneiss (more brittle).

Geology within MFS Faido

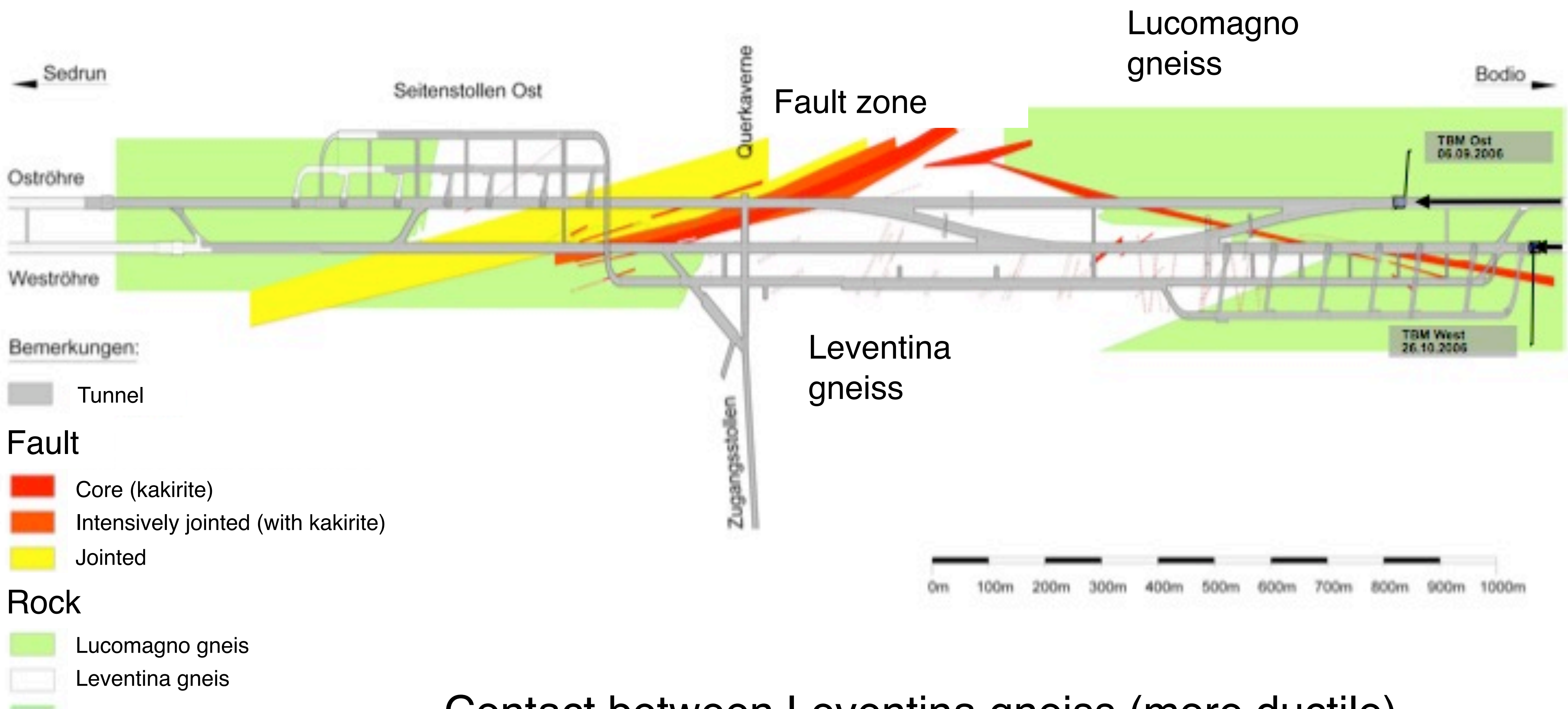

Contact between Leventina gneiss (more ductile) and Lucomagno gneiss (more brittle).

Fault zone with a dip of 80^0 and a strike of 15^0 to the tunnel axis.

Geology within MFS Faido

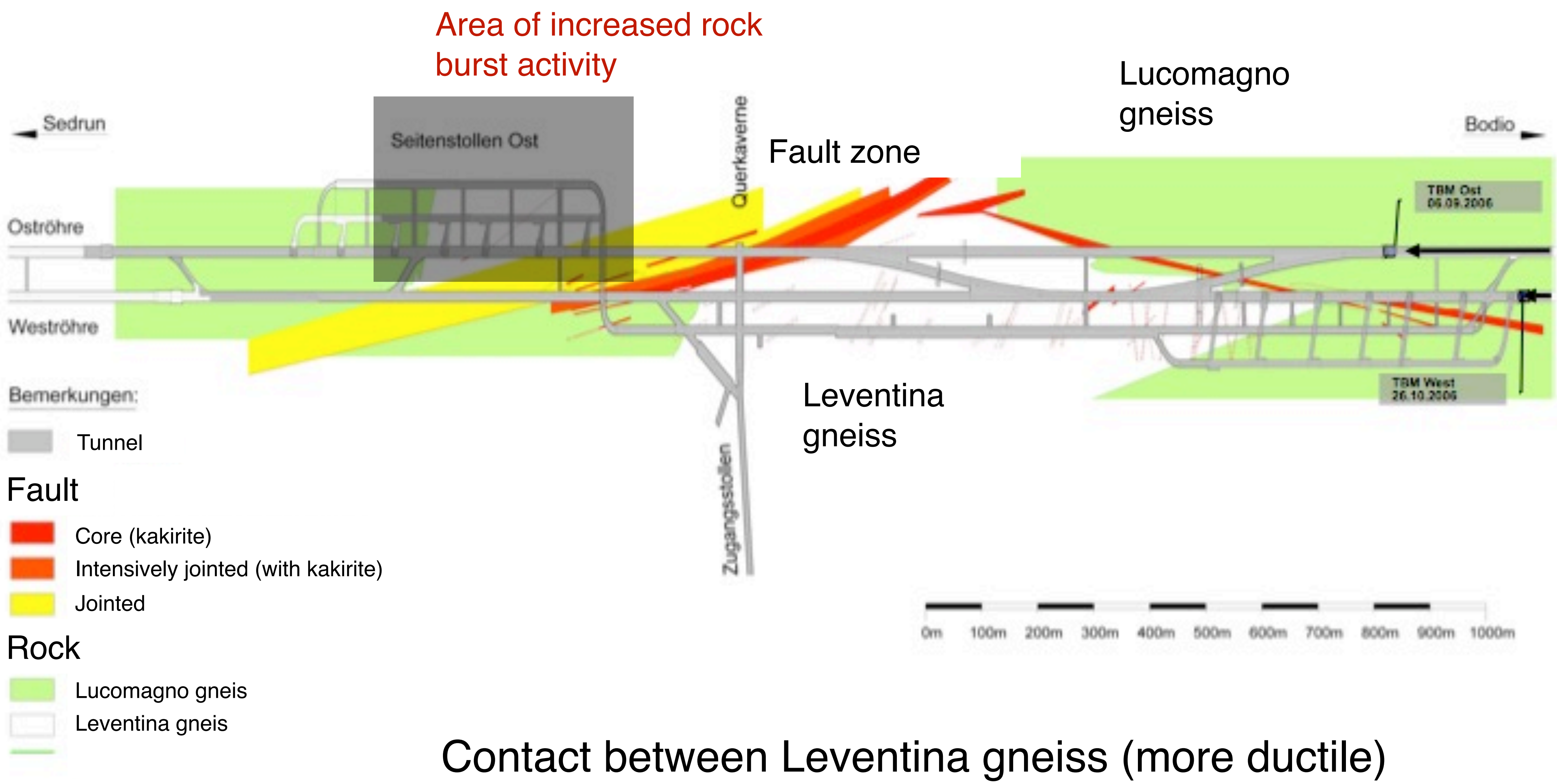

Contact between Leventina gneiss (more ductile) and Lucomagno gneiss (more brittle).

Fault zone with a dip of 80⁰ and a strike of 15⁰ to the tunnel axis.

Strong rock bursts during excavation work

Mainly at the active mining face but also in the back area.

75 % occurred within the first 3 hours after blasting.

Some strong rock bursts could be associated with small earthquakes recorded by the SED, e.g. rock burst on November 15, 2005, correlated with a Ml=1.5 earthquake.

Photo: T. Eppler, Amberg Engineering

Goals of study

Goals of study

- Monitor seismicity with a dense local network in order to estimate accurate locations (error < 50 m in epicenter and < 200 m in focal depth),

Goals of study

- Monitor seismicity with a dense local network in order to estimate accurate locations (error < 50 m in epicenter and < 200 m in focal depth),

- Investigate processes that could generate the observed seismicity (correlation with rock bursts, tectonic activity, induced earthquakes),

Goals of study

- Monitor seismicity with a dense local network in order to estimate accurate locations (error < 50 m in epicenter and < 200 m in focal depth),
- Investigate processes that could generate the observed seismicity (correlation with rock bursts, tectonic activity, induced earthquakes),
- Assess seismic hazard associated with the seismicity during construction and future operation.

Goals of study

- Monitor seismicity with a dense local network in order to estimate accurate locations (error < 50 m in epicenter and < 200 m in focal depth),
- Investigate processes that could generate the observed seismicity (correlation with rock bursts, tectonic activity, induced earthquakes),
- Assess seismic hazard associated with the seismicity during construction and future operation.

To reach these goals a contract was given by AlpTransit Gotthard AG (ATG) to SED for seismic monitoring. Furthermore, the working group Mikrobeben AG was established consisting of representatives of ATG, Amberg Engineering AG, Pöyry AG, Lombardi AG, Basler & Hofmann, and SED.

Seismic network AlpTransit Faido

9 surface stations (incl. SDSNet station FUSIO) and 2 tunnel stations.

Design consists of two “rings” of stations with 1 km and 10 km radius.

Real-time data transmission to ETHZ and integration to existing data processing and alarming at SED.

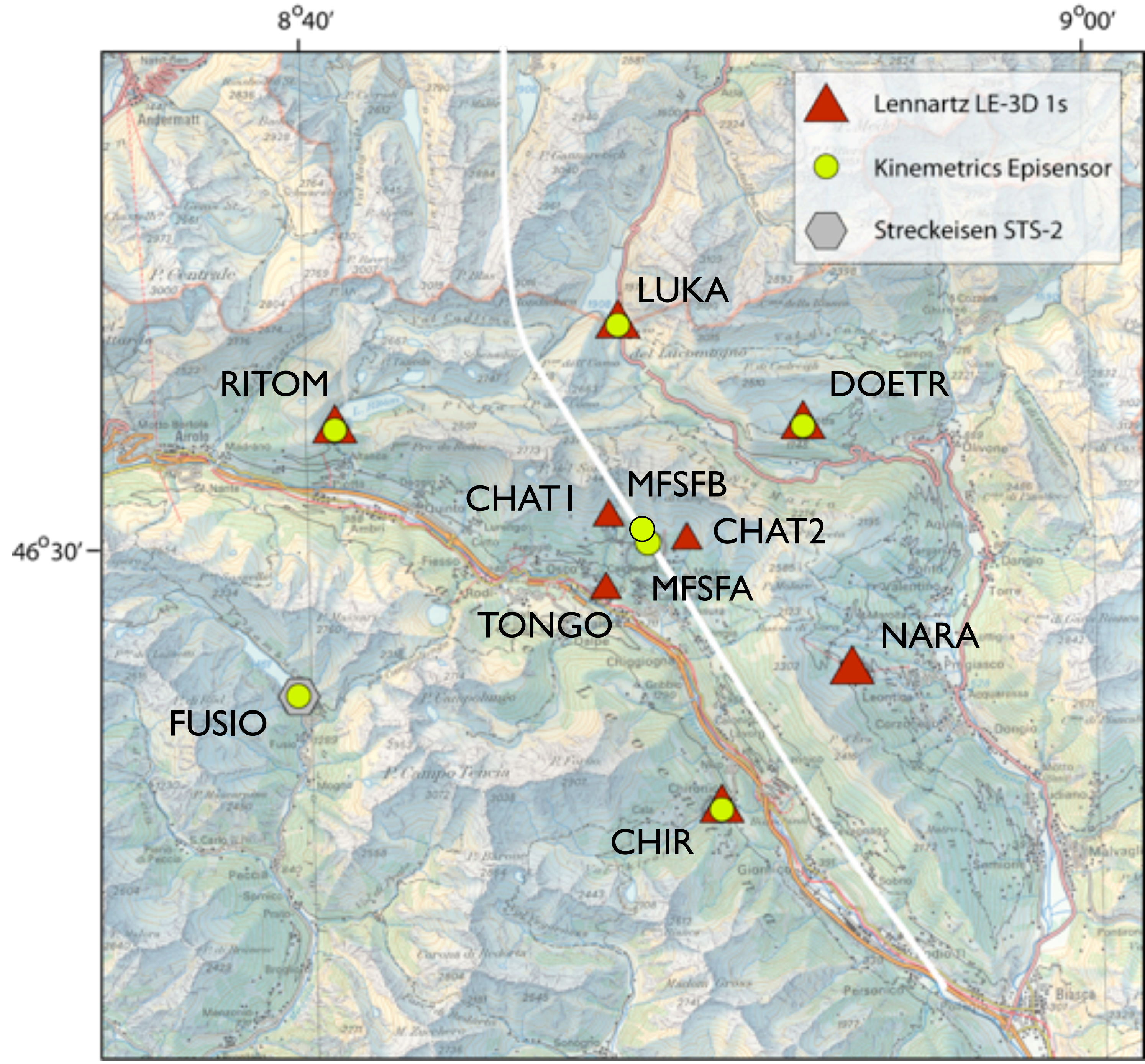

Seismic network AlpTransit Faido

9 surface stations (incl. SDSNet station FUSIO) and 2 tunnel stations.

Design consists of two “rings” of stations with 1 km and 10 km radius.

Real-time data transmission to ETHZ and integration to existing data processing and alarming at SED.

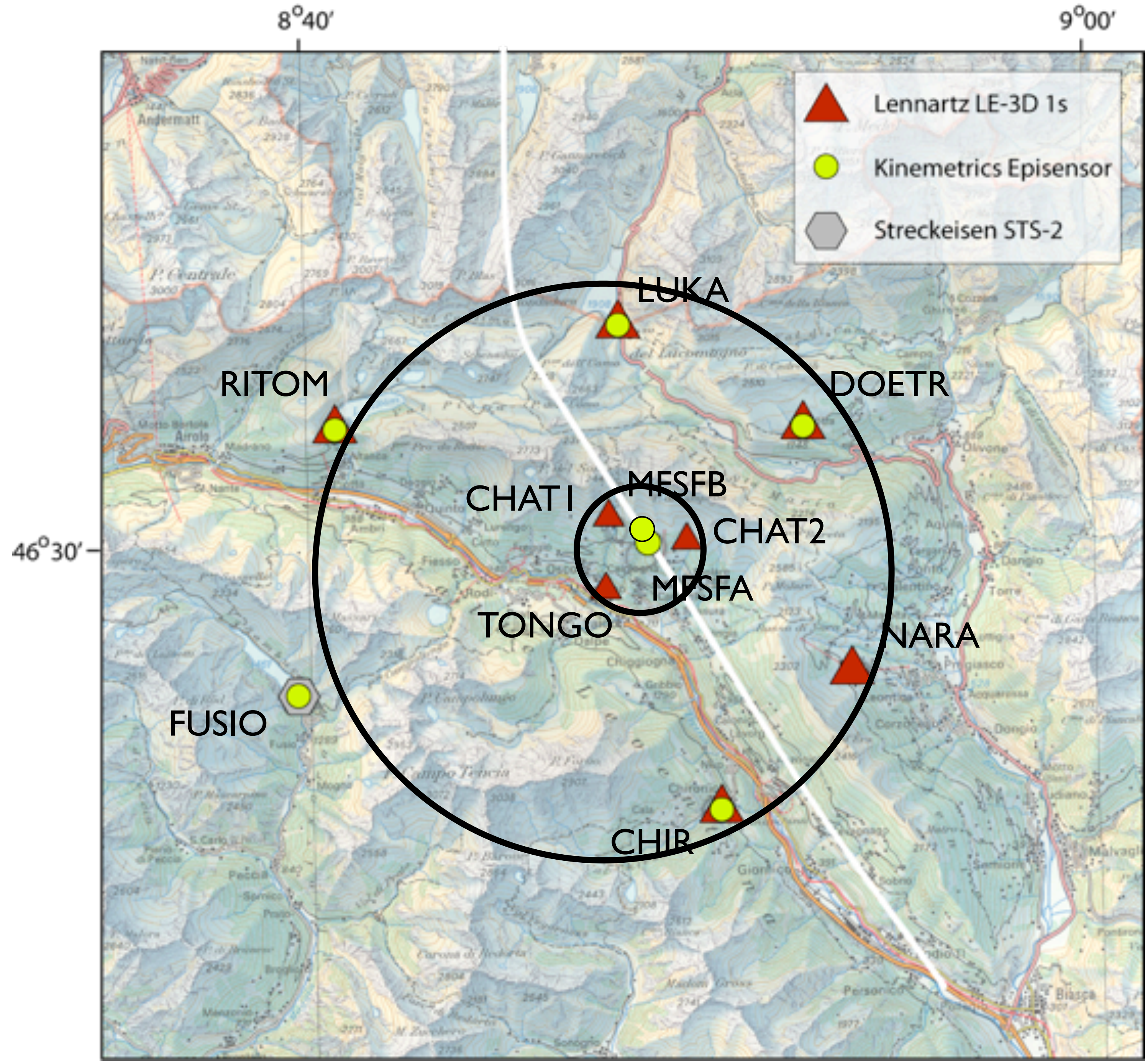

Seismic network AlpTransit Faido

Station DOETR at Alp Doetra

Stations were installed at sites with existing infrastructure (telephone and electricity) to allow real-time data transmission.

Seismic network AlpTransit Faido

Station MFSFA inside MFS Faido

Data transmission via fiber-optic cable to control center at tunnel entrance; from there through ADSL (telephone line) to ETHZ.

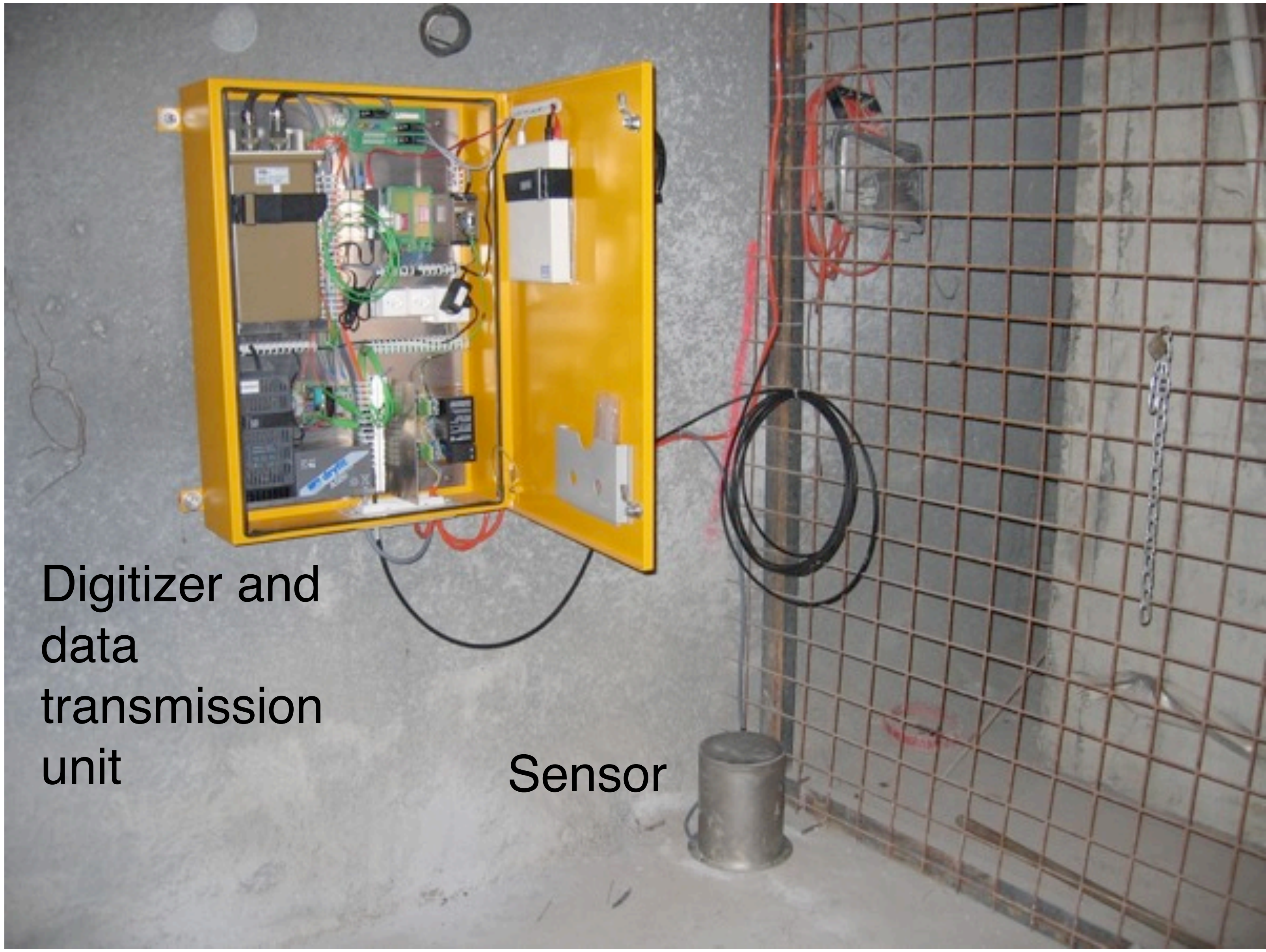

Determination of earthquake locations

Earthquakes were relocated using a non-linear probabilistic solution (NonLinLoc).

Includes a full description of the location uncertainties (represented by the 68% confidence error ellipsoid).

Hypocenter location of a Ml=1.9 earthquake recorded only at 10 SDSNet station using 3-D P-wave velocity model for Switzerland.

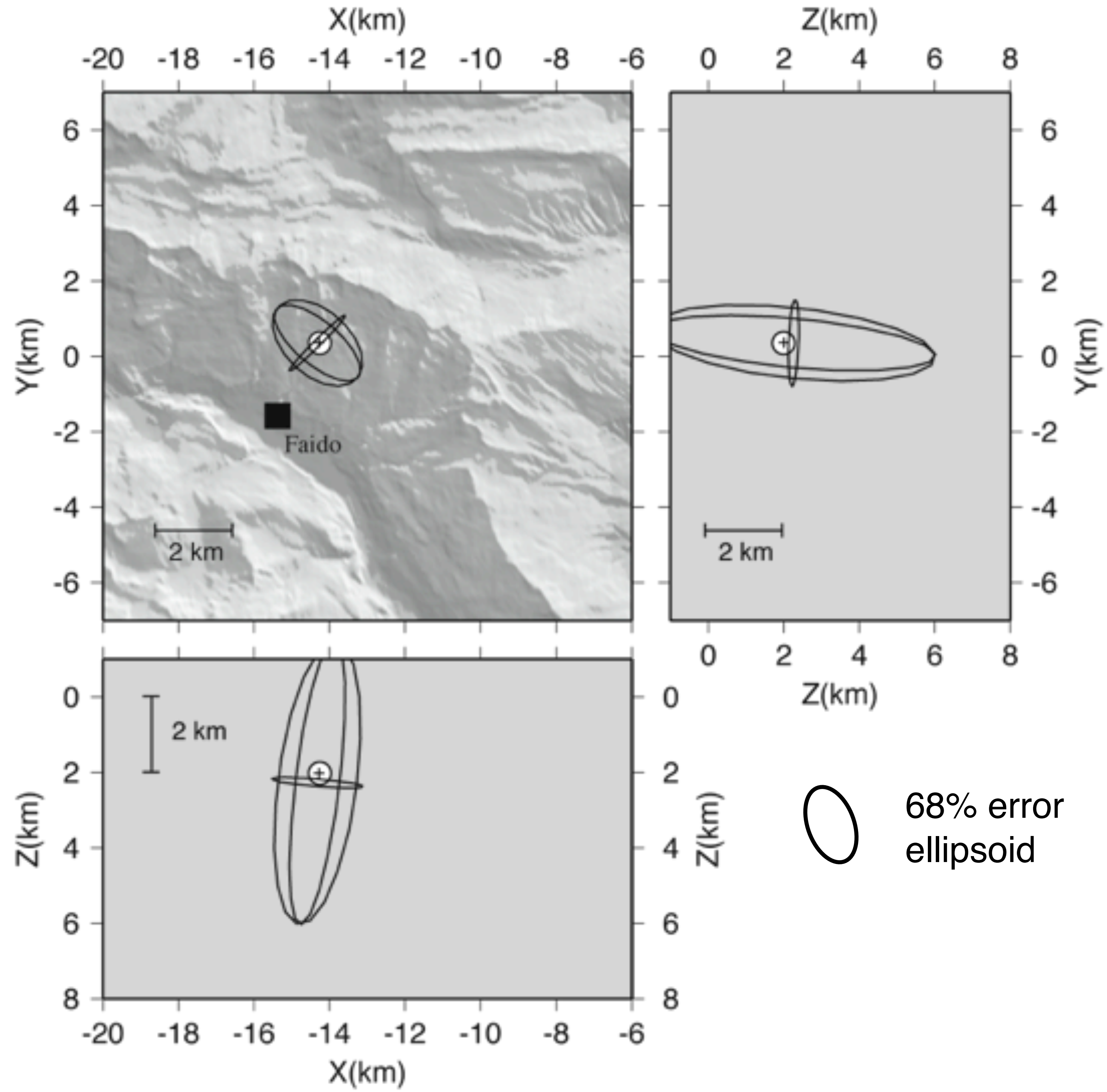

Determination of earthquake locations

Same earthquake but relocated using SDSNet and Alptransit stations.

Error are reduced by a factor of ~2 in epicenter and by a factor of ~4 in focal depth.

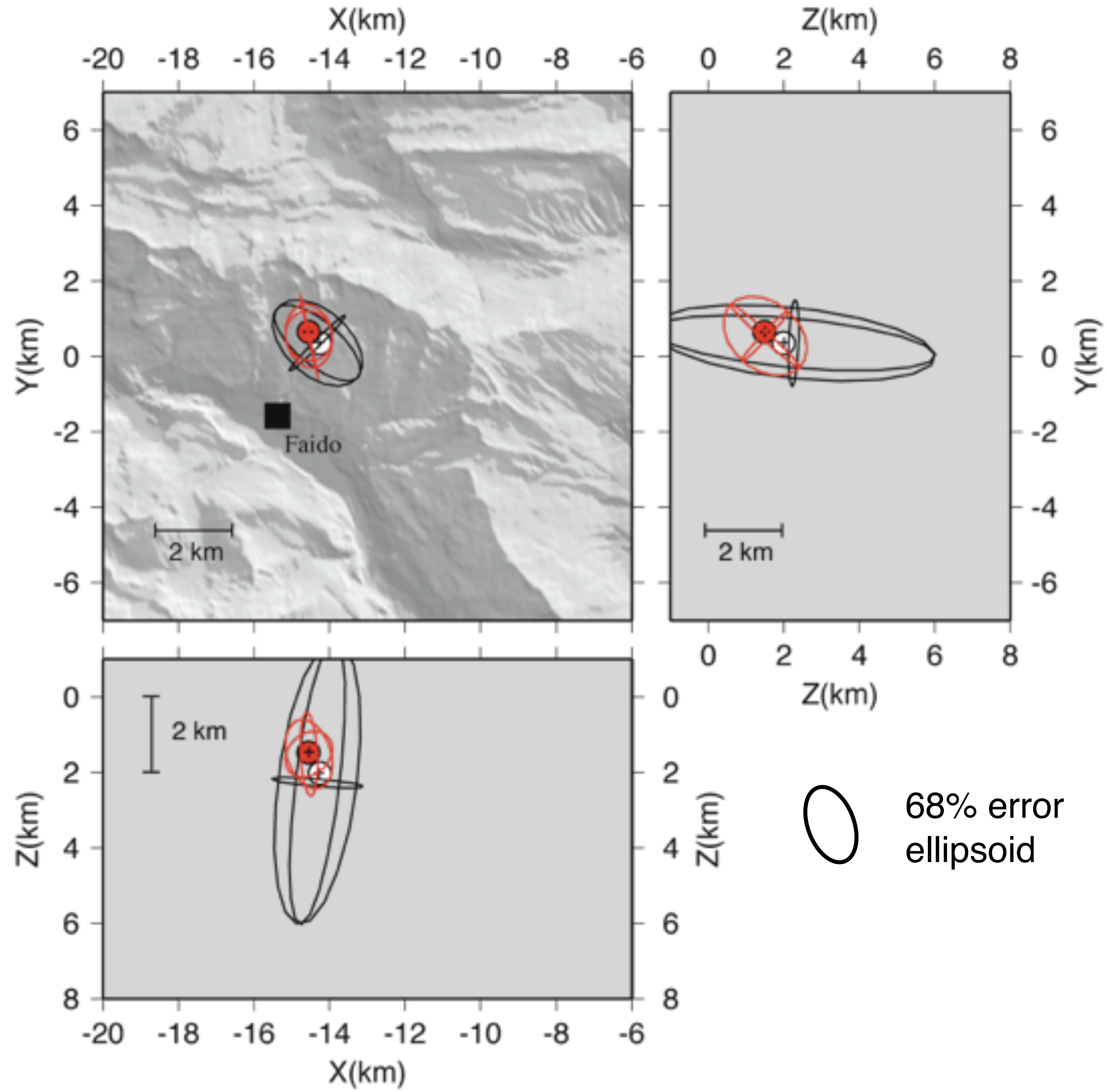

Determination of earthquake locations

Same earthquake but relocated using SDSNet and Alptransit stations.

Error are reduced by a factor of ~2 in epicenter and by a factor of ~4 in focal depth.

Using 3-D P-wave velocity model focal depths are 2 km below tunnel!

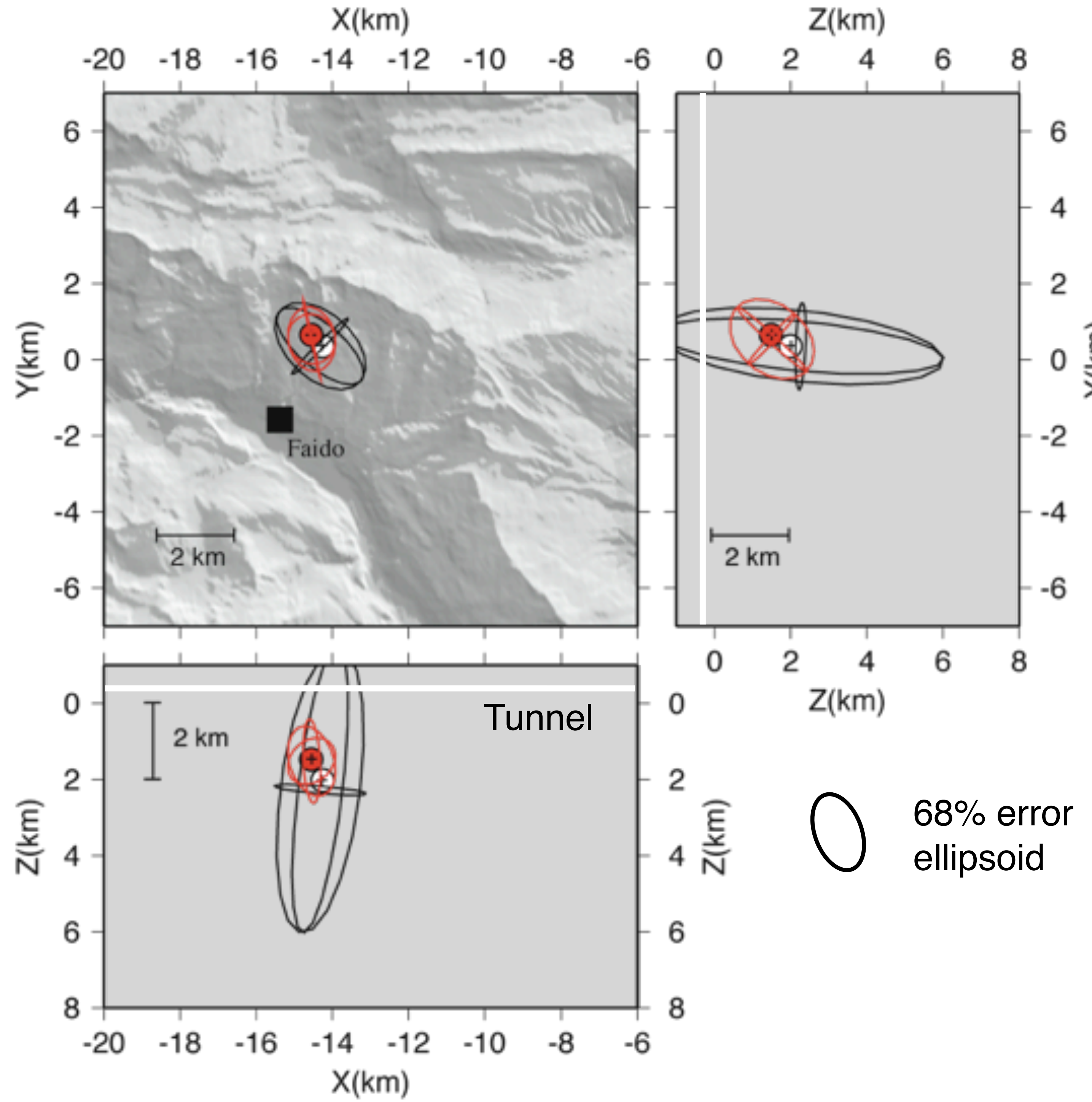

Calibration shot

A calibration shot of 100 Kg was used to calibrate seismic P-wave velocities.

Shot time was recorded by a sensor next to the shot borehole.

Photo: T. Eppler, Amberg Engineering

Calibration shot

Measured P-wave velocities vary by more than 10 % !

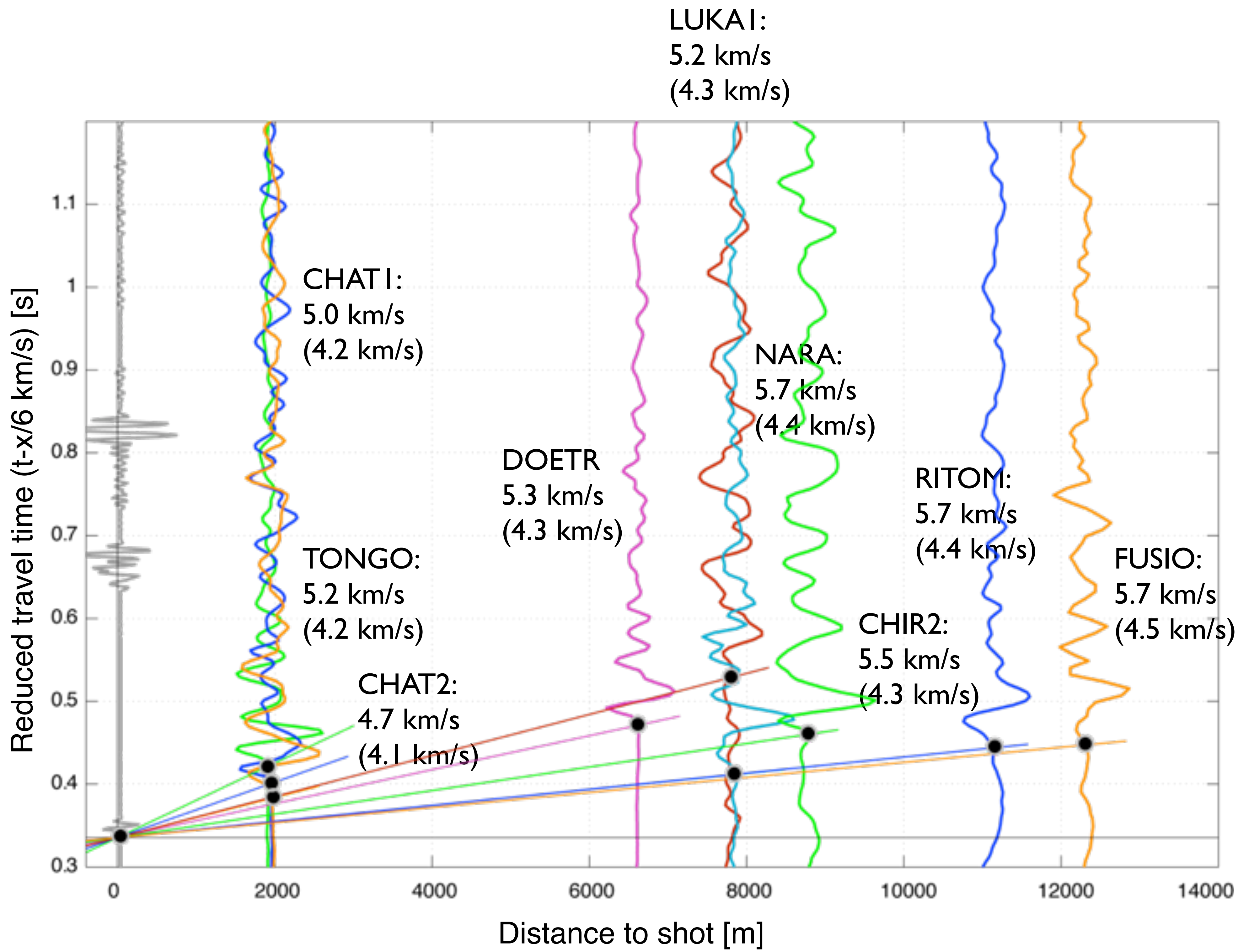

Calibration shot

Measured P-wave velocities vary by more than 10 % !

P-wave velocities of the 3D model are too slow and do not show local variations as compared to true velocities.

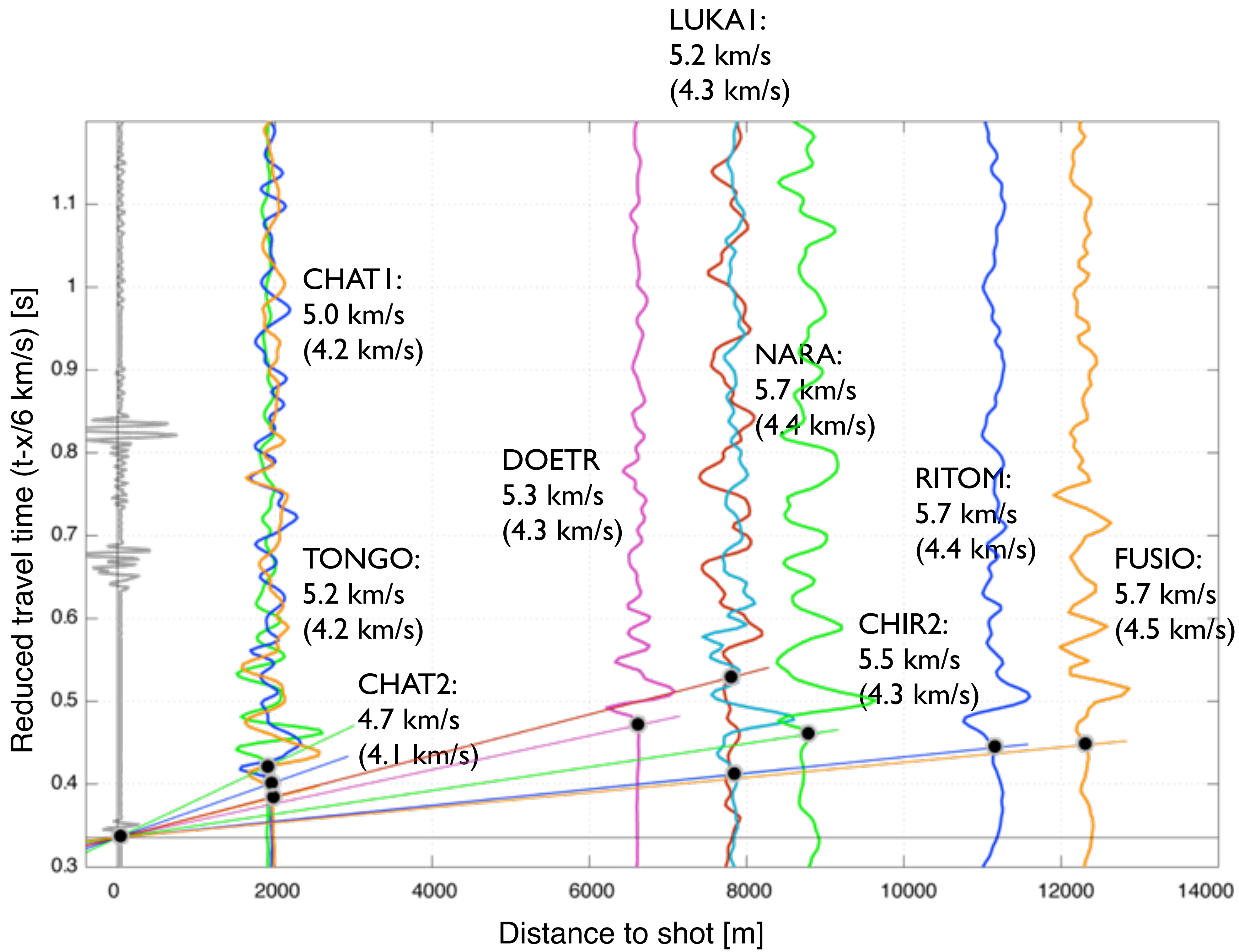

Relocation of calibration shot

mislocation (compared to true location)

diffx: 200 m

diffy: 20 m

diffz: 2100 m

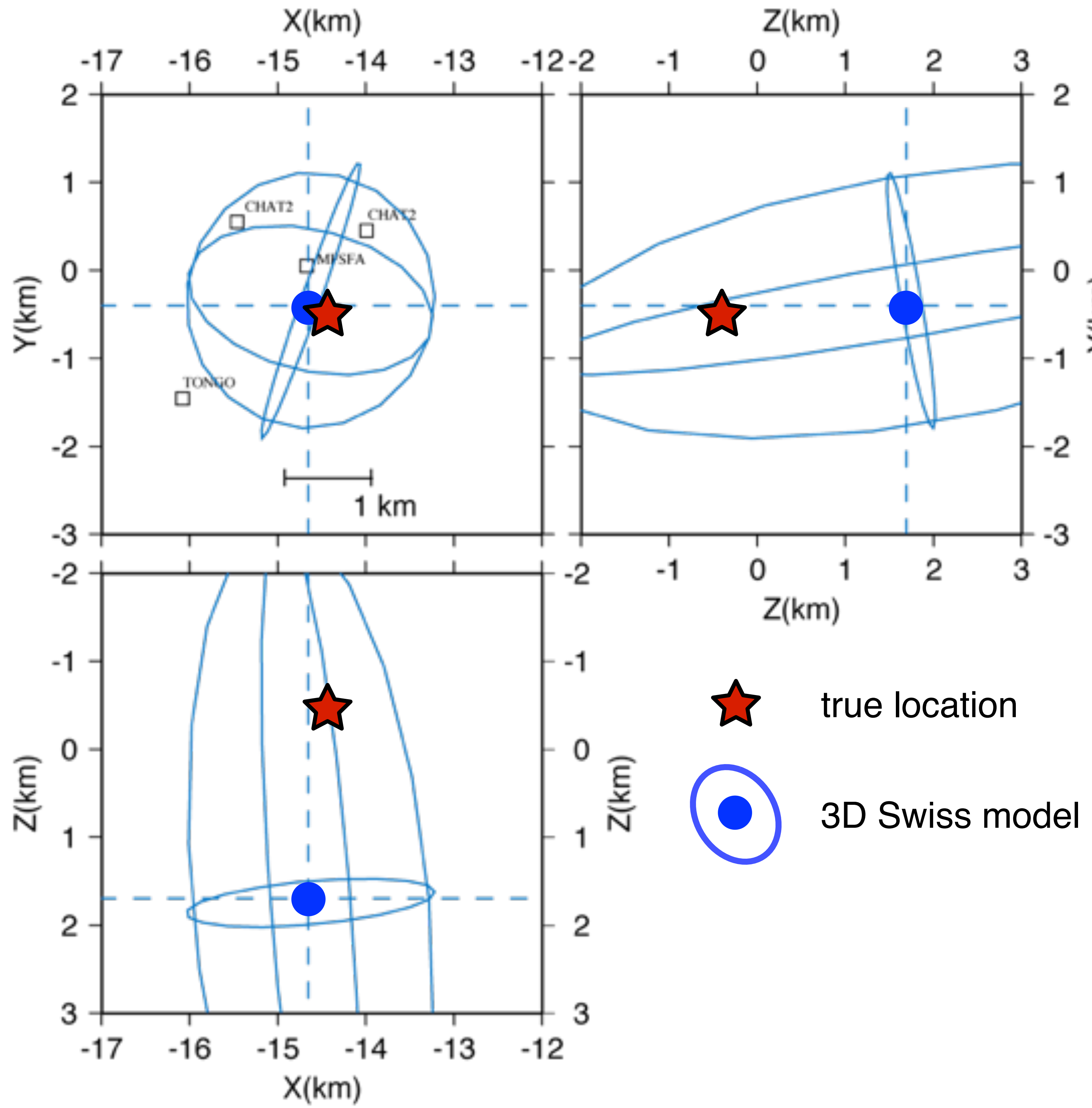

Relocation of calibration shot

mislocation (compared to true location)

diffx: 200 m

diffy: 20 m

diffz: 2100 m

mislocation (compared to true location)

diffx: 25 m

diffy: 70 m

diffz: 250 m

Location accuracy of 75 m in epicenter and 250 m in depth!

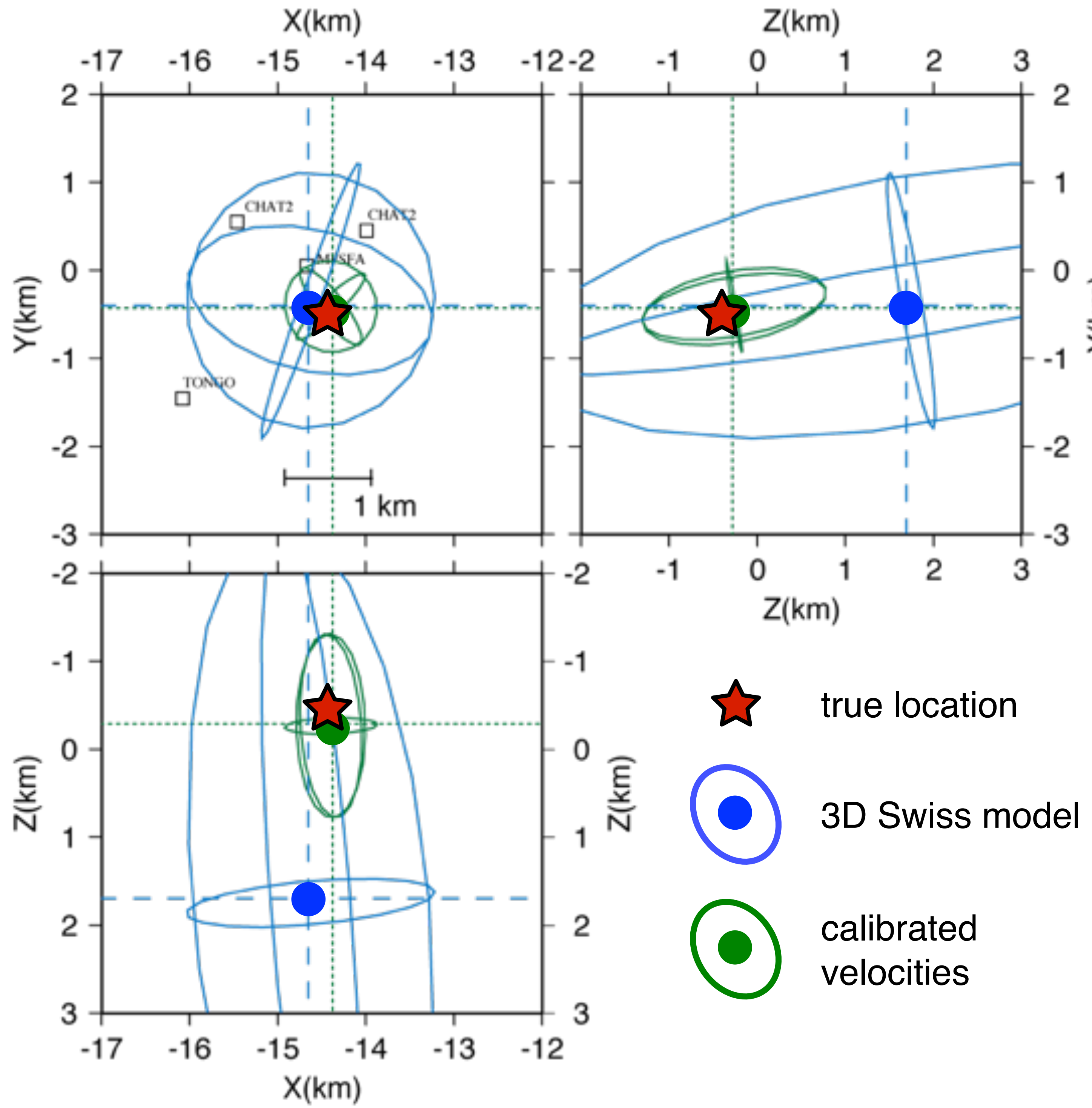

Temporal evolution (Oct. 2005 - Dec. 2007)

In total 112 earthquakes were recorded.

Local magnitudes range from -0.9 to 2.4.

Decay (in numbers and magnitudes) of seismicity over time.

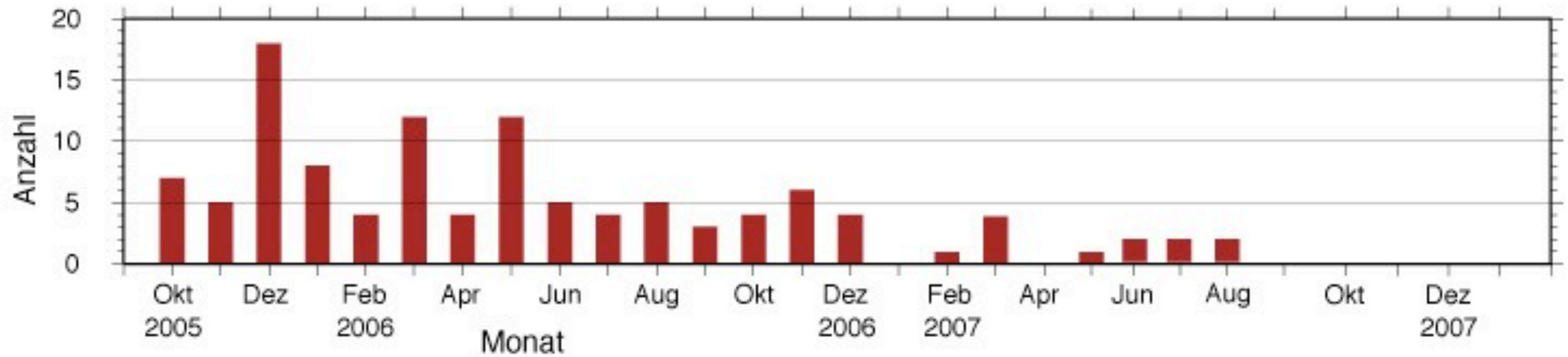

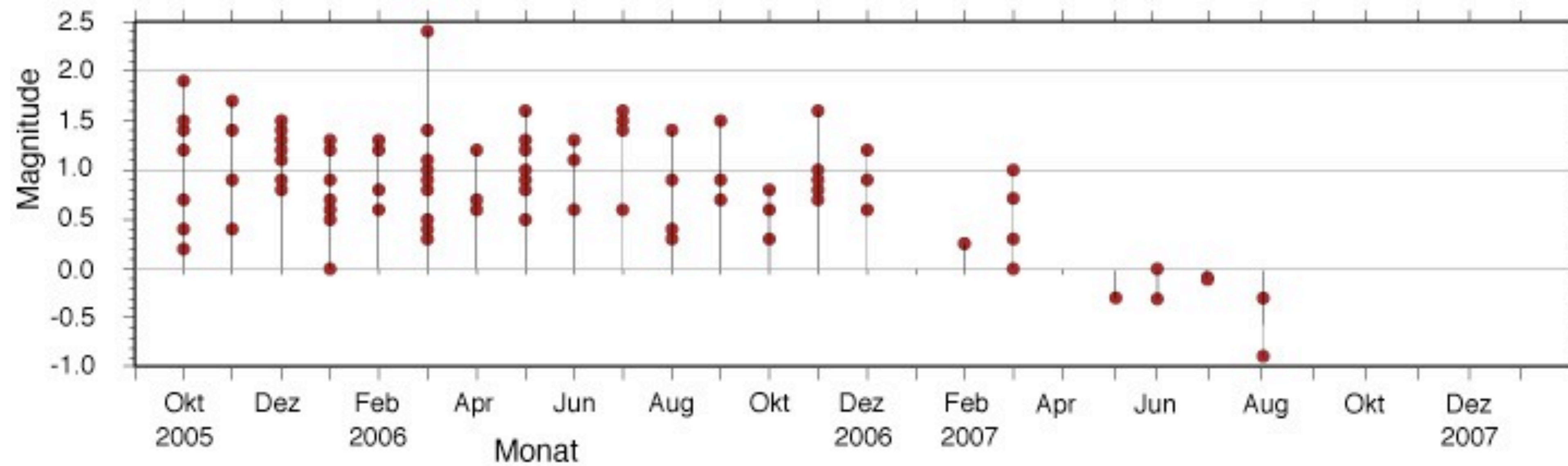

Temporal evolution (Oct. 2005 - Dec. 2007)

In total 112 earthquakes were recorded.

Local magnitudes range from -0.9 to 2.4.

Decay (in numbers and magnitudes) of seismicity over time.

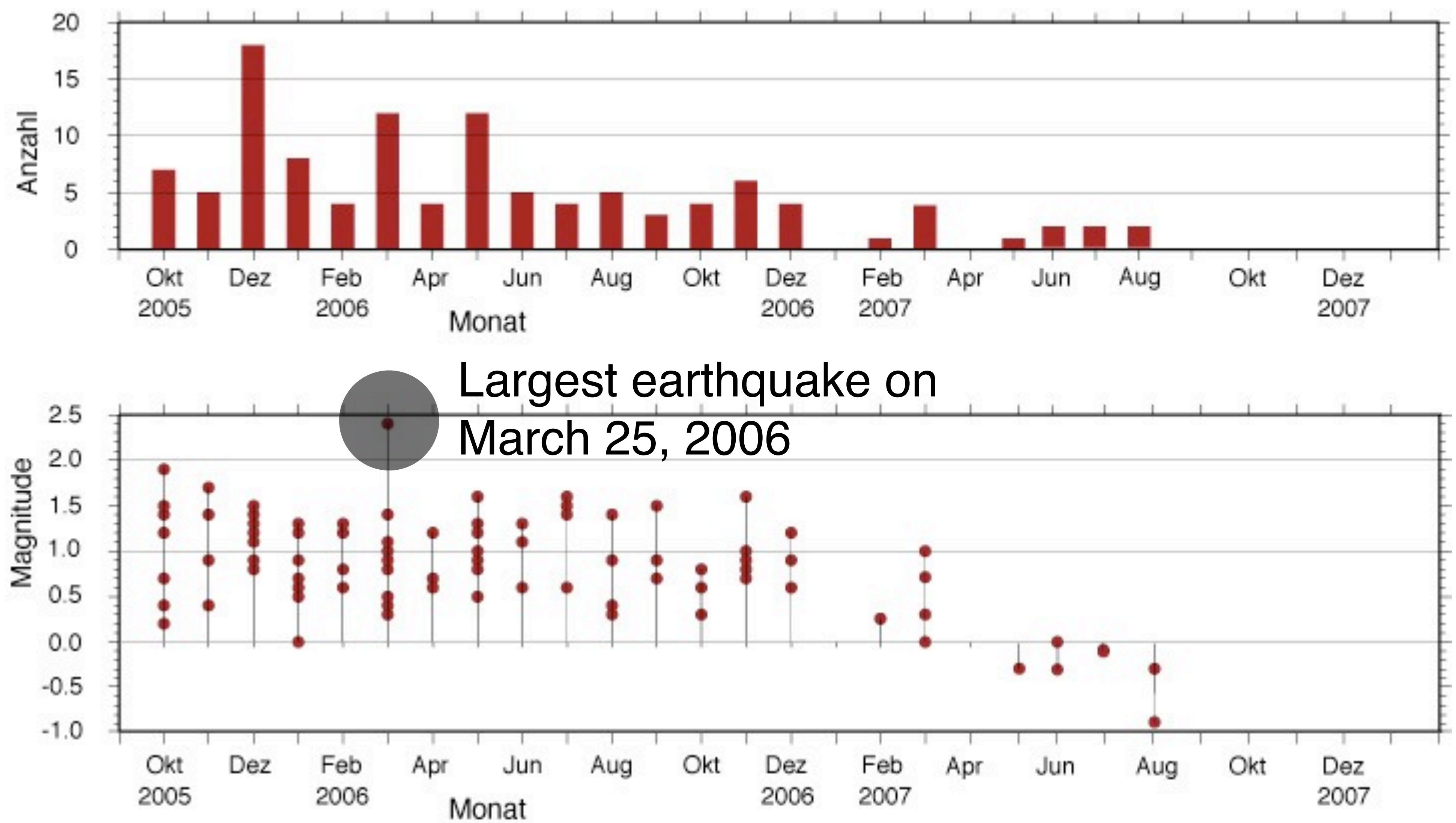

Earthquake of March 25, 2006

With Ml=2.4 strongest earthquake in the series.

Was widely felt in nearby villages.

Caused damage in the tunnel (mainly uplift of floor).

Caused intensive media interest.

Photo: T. Eppler, Amberg Engineering

Earthquake of March 25, 2006 (cont.)

The large number of observations allowed to compute a reliable focal mechanism.

Strike of 281^0 and dip of 83^0 are in good agreement with geology.

Earthquake occurred likely on or to close to mapped fault zone.

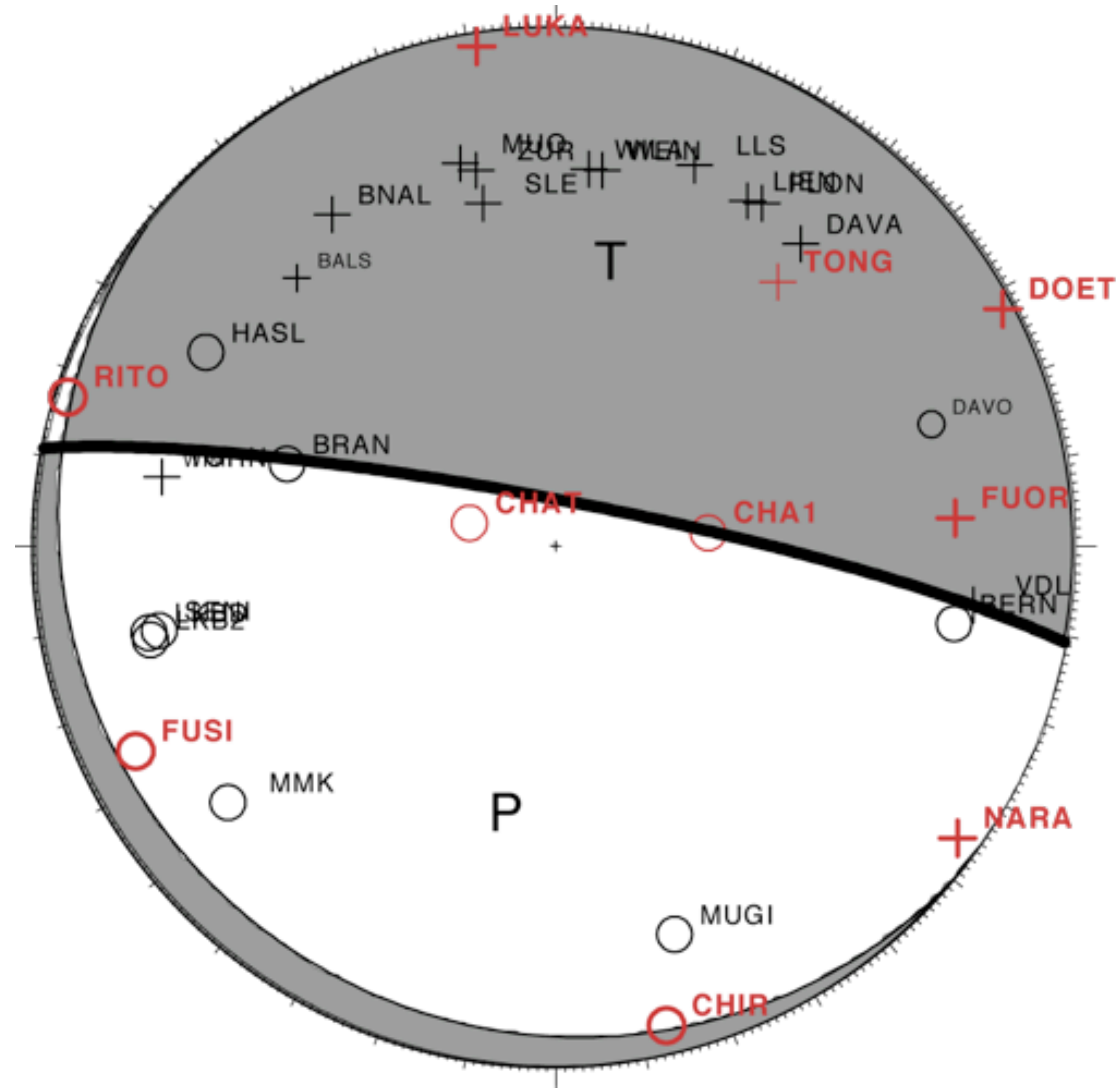

Epicenter locations

Only well-locatable earthquakes are shown (GAP < 160^0, max. length of error ellipsoid < 1.0 km)

Earlier earthquakes (Dec. 2005 to Feb. 2006) tend to occur in the southern part.

Earthquakes occurred mainly to the east of the fault zone in the Lucomagno gneiss.

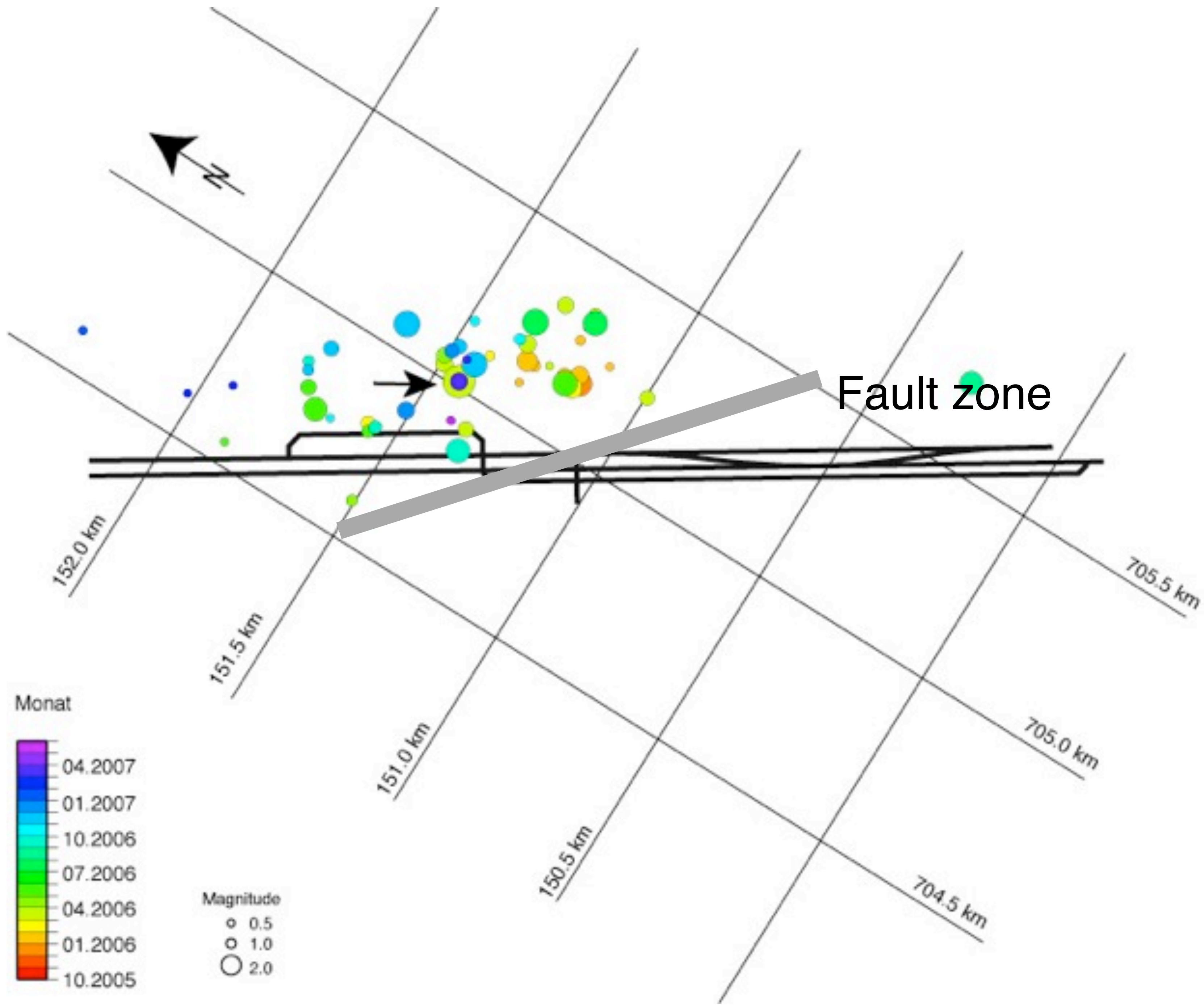

Waveform similarities

We observed clusters of earthquakes with very similar waveforms.

Example shows waveforms at station DOETR between January 2006 and April 2006 (horizontal component EHE, BP 1- 10 Hz filtered)

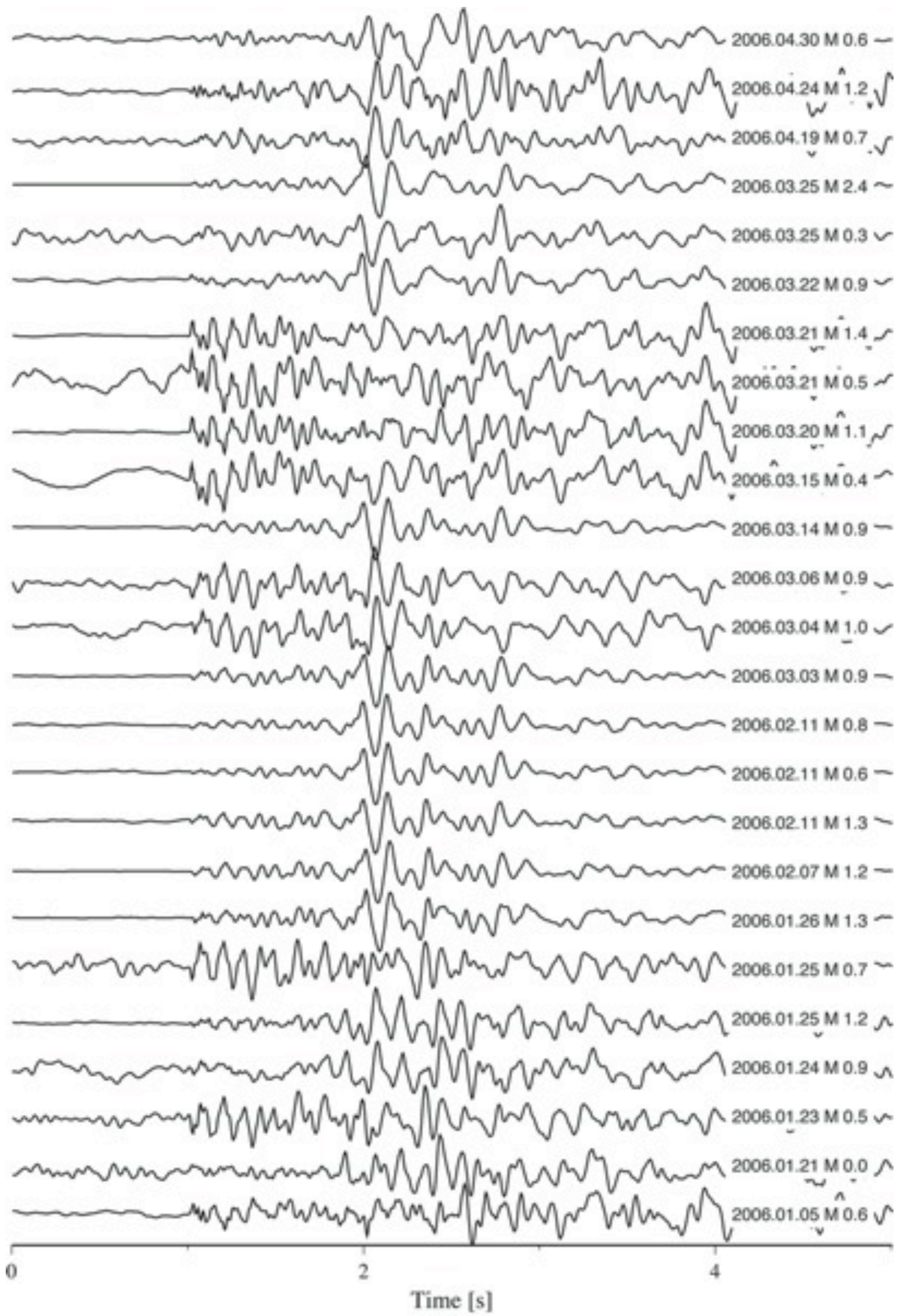

Waveform similarities (cont.)

Systematic analysis of waveform similarities at station DOETR yield 12 clusters.

Ml=2.4 earthquake of March 25, 2006, is part of cluster 11, the largest cluster.

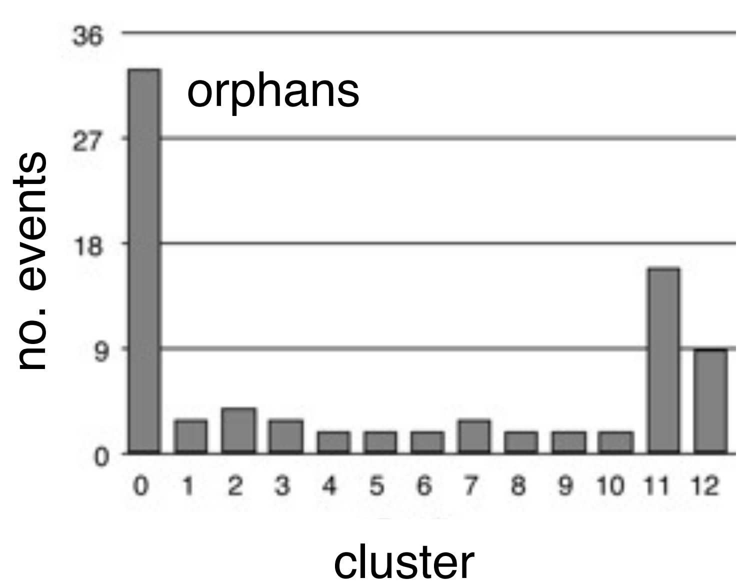

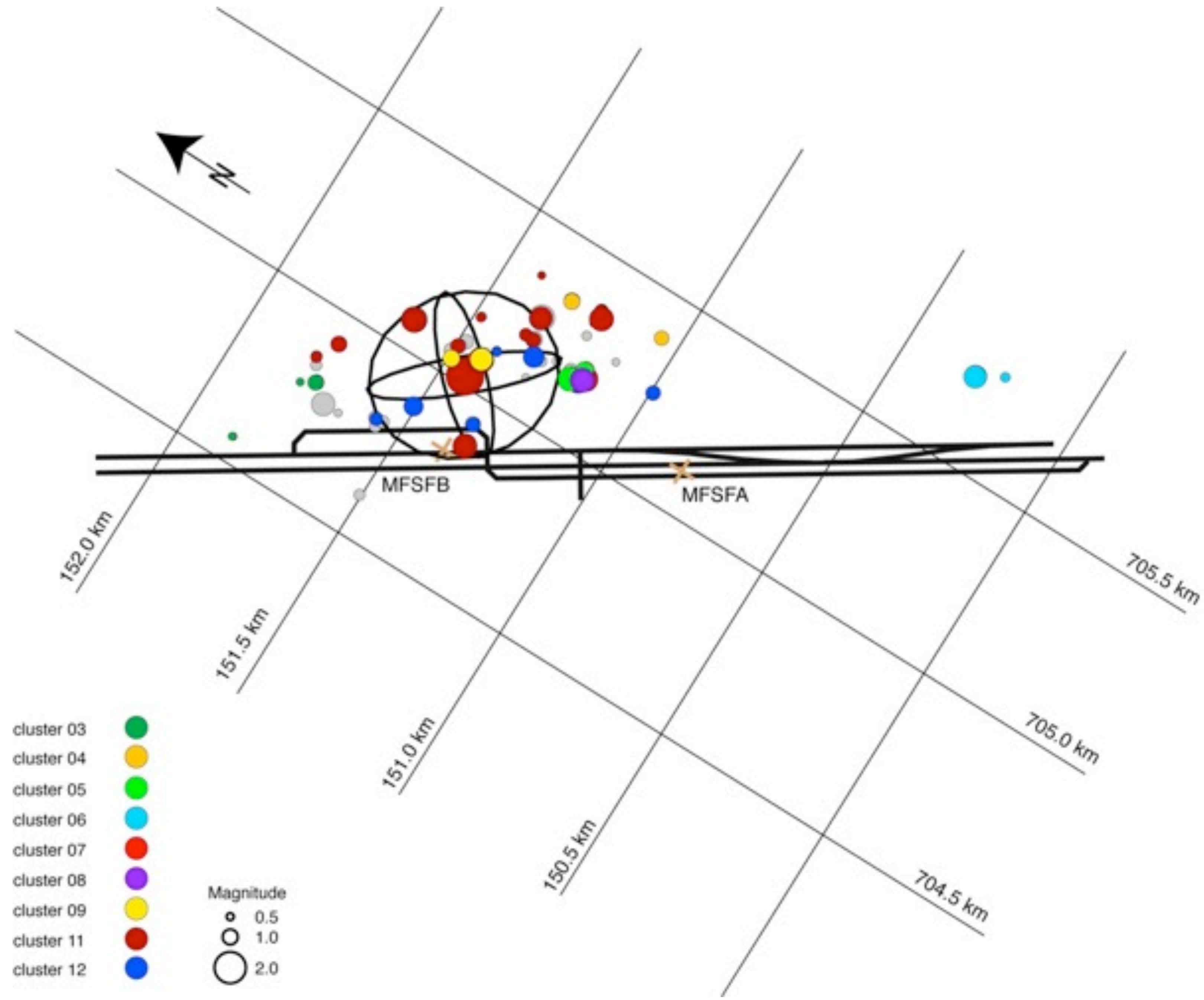

Waveform similarities (cont.)

Systematic analysis of waveform similarities at station DOETR yield 12 clusters.

Ml=2.4 earthquake of March 25, 2006, is part of cluster 11, the largest cluster.

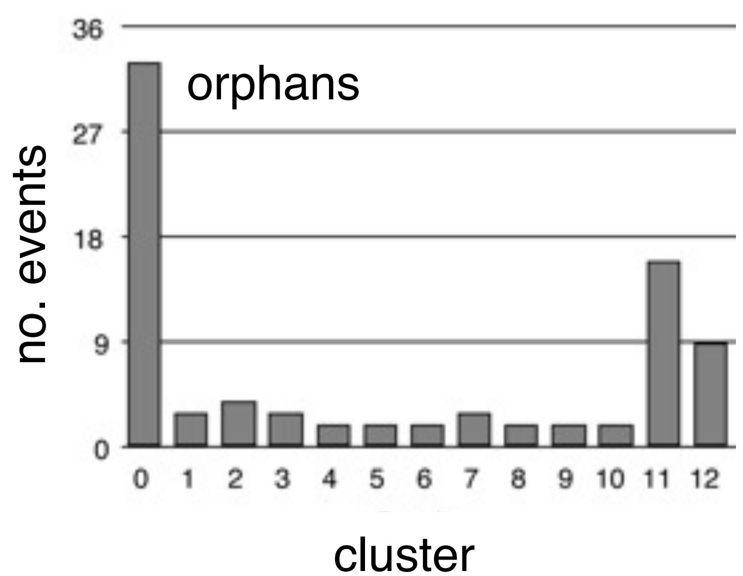

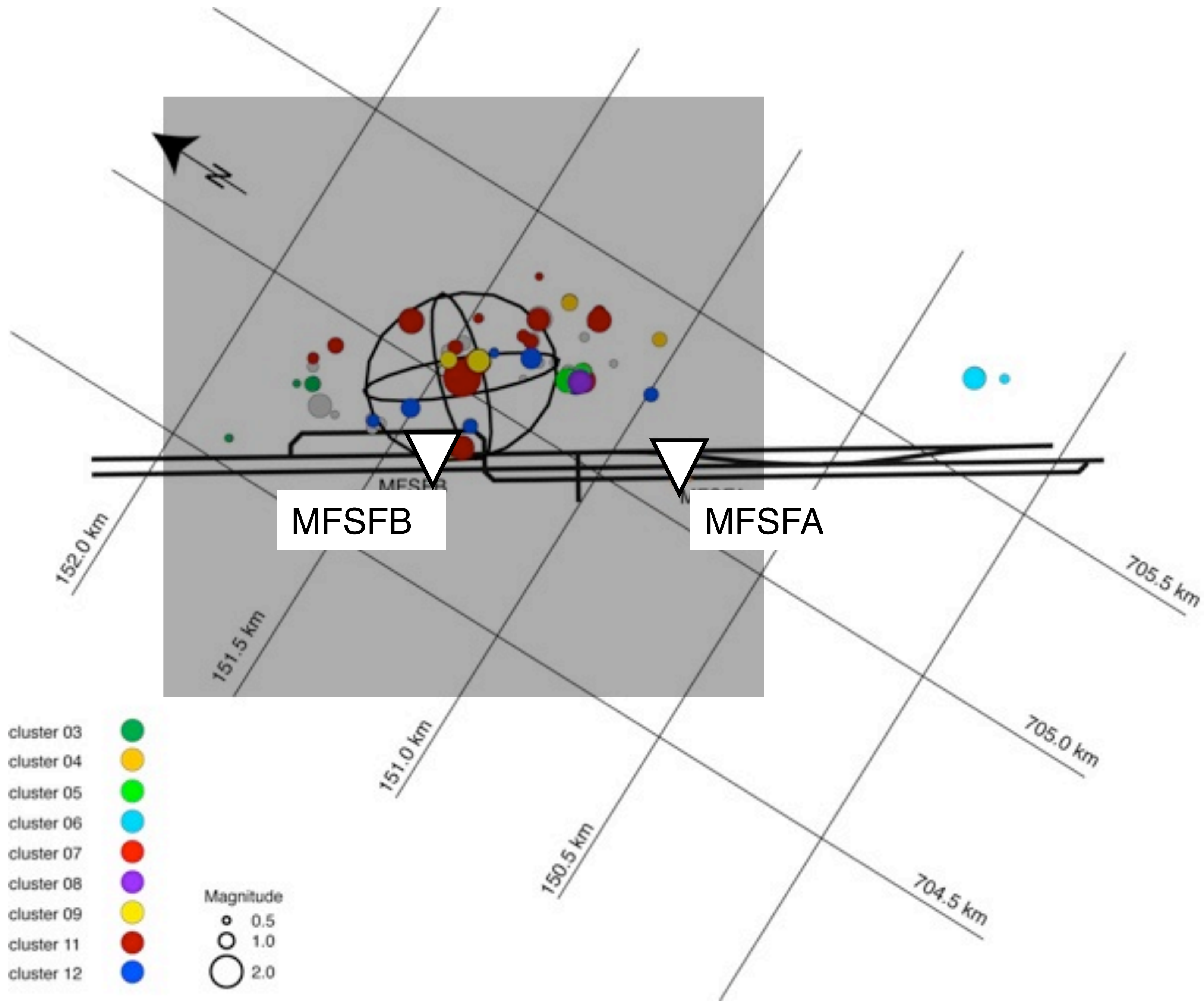

Improved pick quality

Improved arrival time picks by cross-correlation measurements (Rowe et al., 2002)

Improvement in pick quality shown for cluster11.

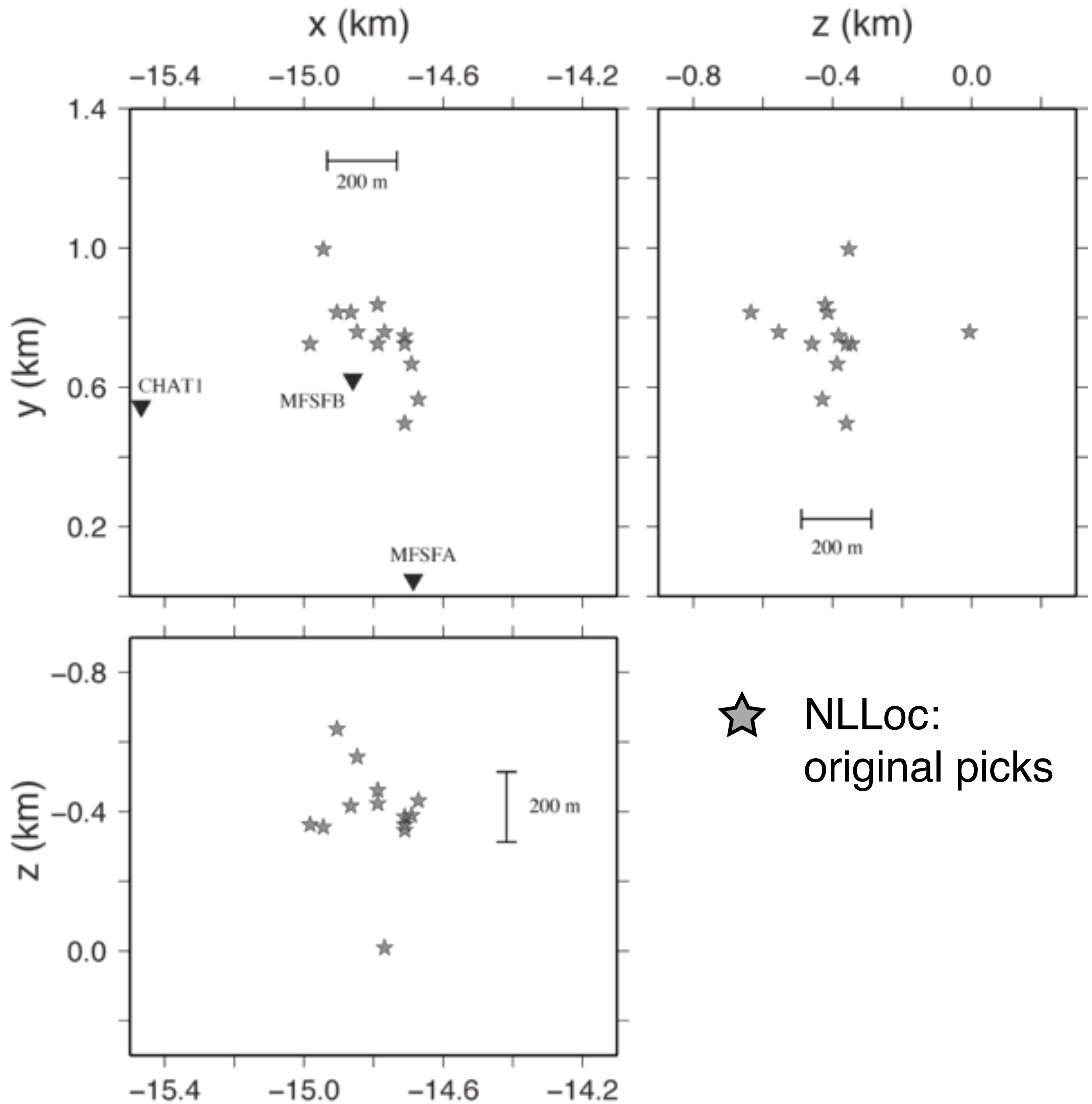

Improved pick quality

Improved arrival time picks by cross-correlation measurements (Rowe et al., 2002)

Improvement in pick quality shown for cluster11.

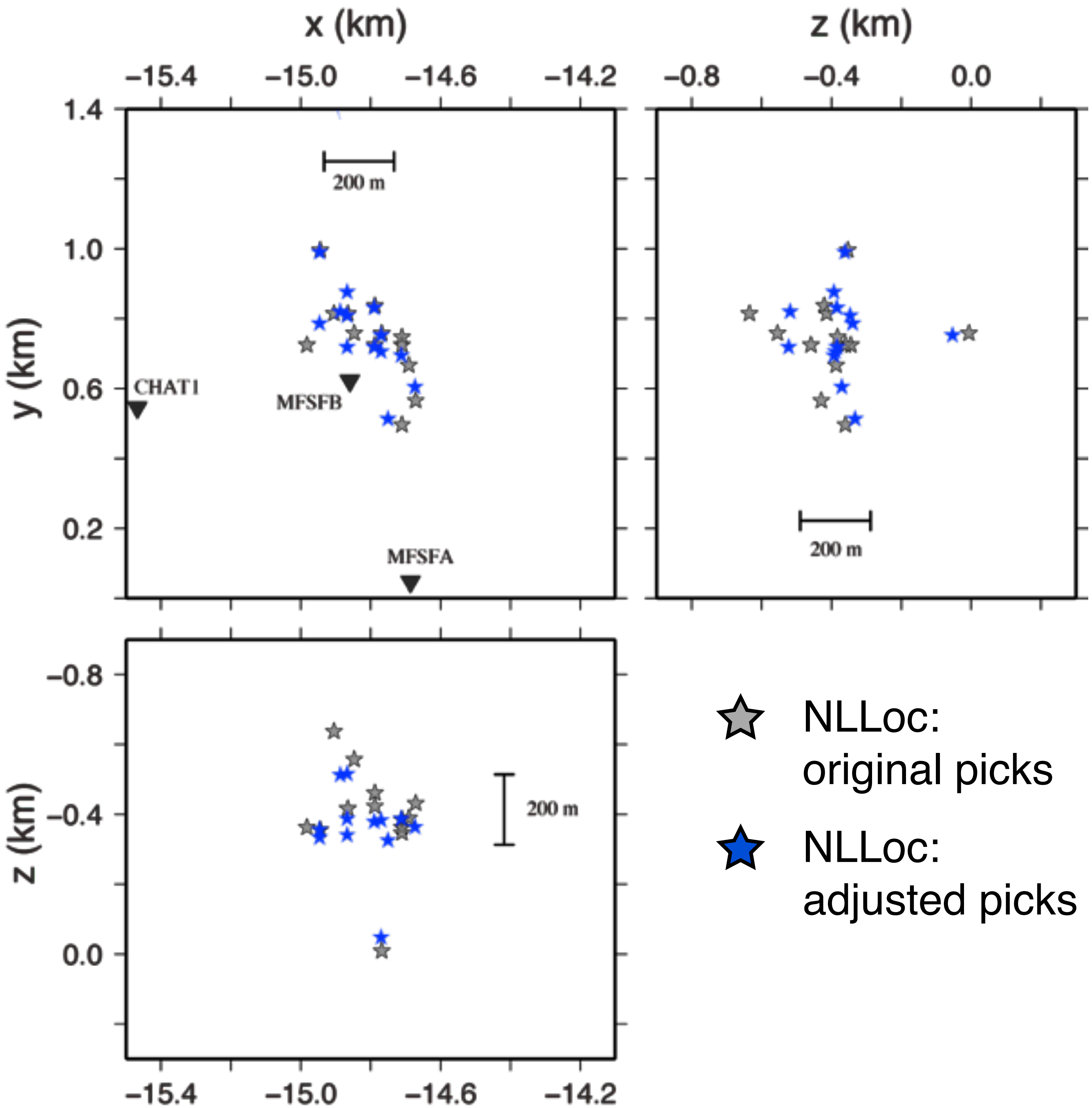

Improved pick quality

Improved arrival time picks by cross-correlation measurements (Rowe et al., 2002)

Improvement in pick quality shown for cluster11.

Error ellipsoids overlap indicating that absolute locations are not significantly different.

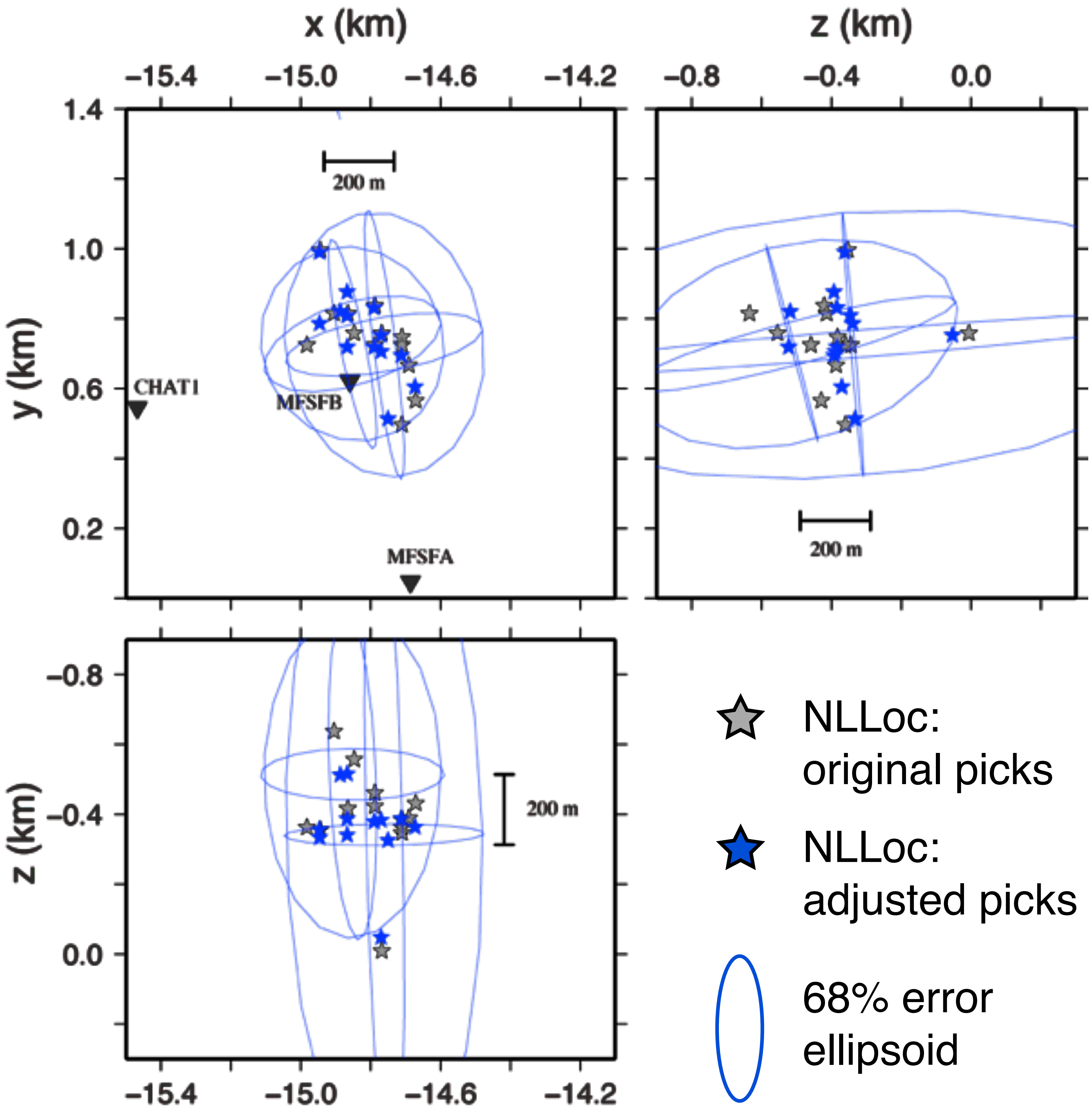

HypoDD relative relocations

HypoDD relative relocations show tighter clustering.

Cross-correlation measurements improve clustering.

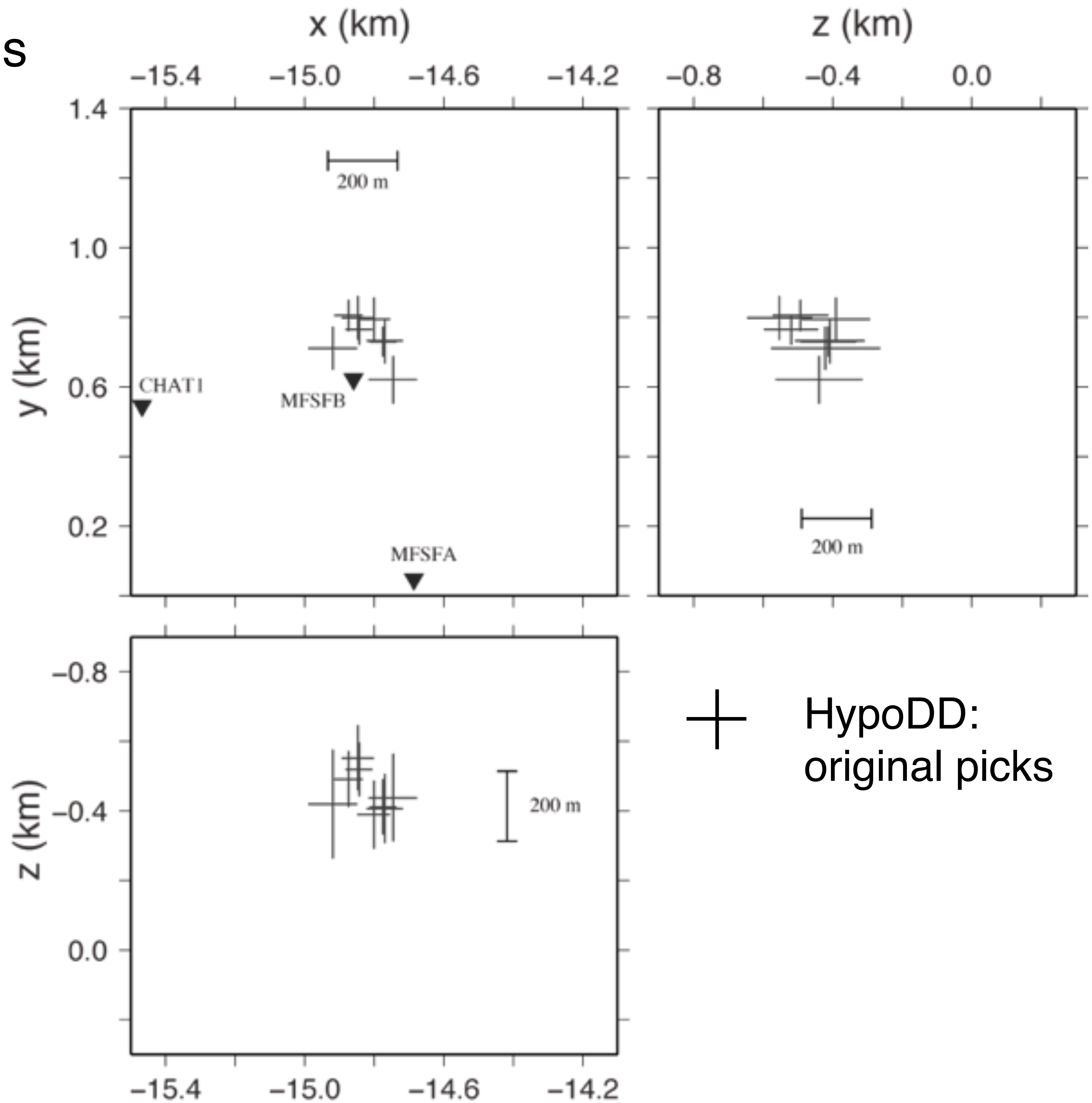

HypoDD relative relocations

HypoDD relative relocations show tighter clustering.

Cross-correlation measurements improve clustering.

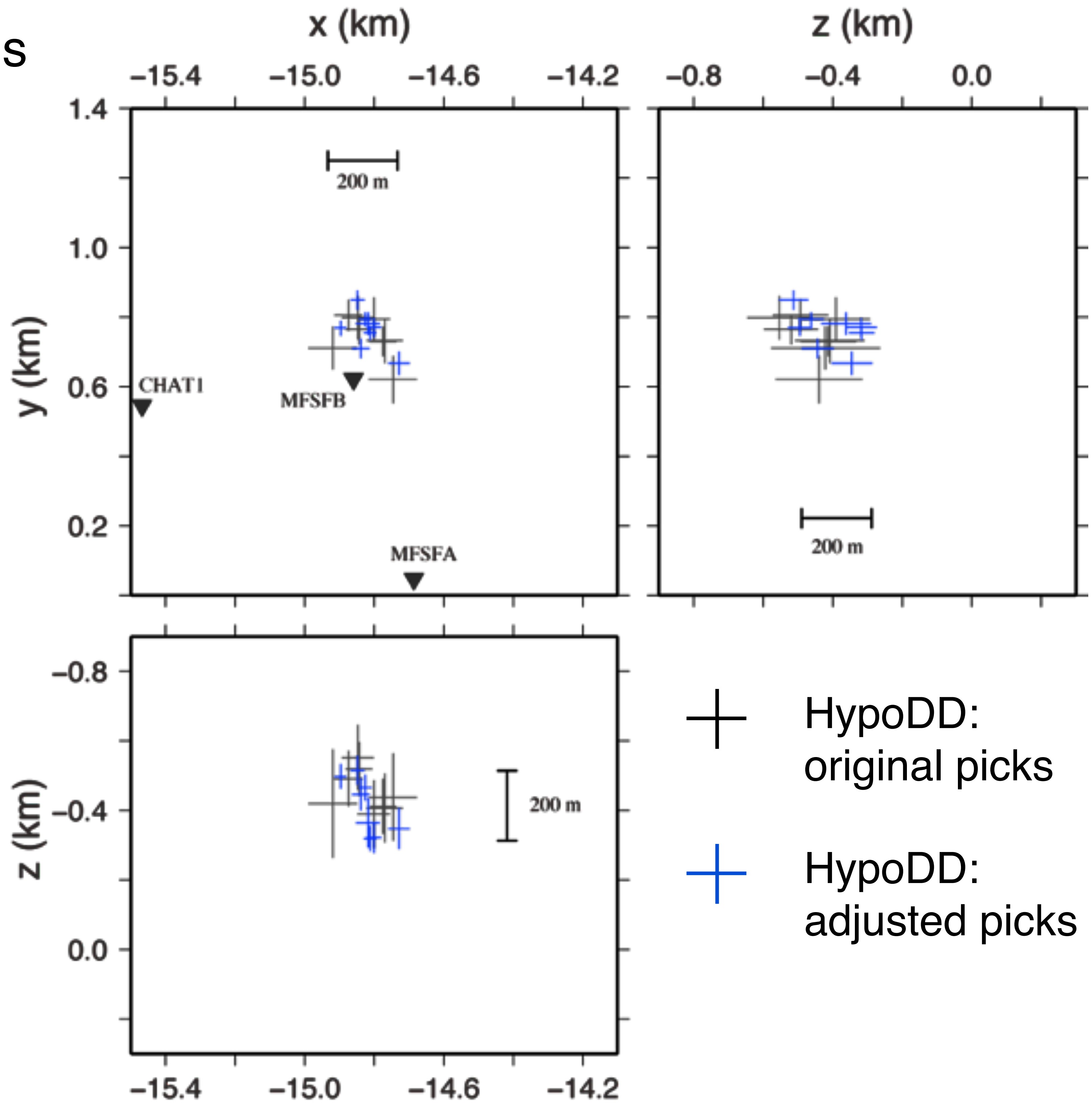

HypoDD relative relocations

HypoDD relative relocations show tighter clustering.

Cross-correlation measurements improve clustering.

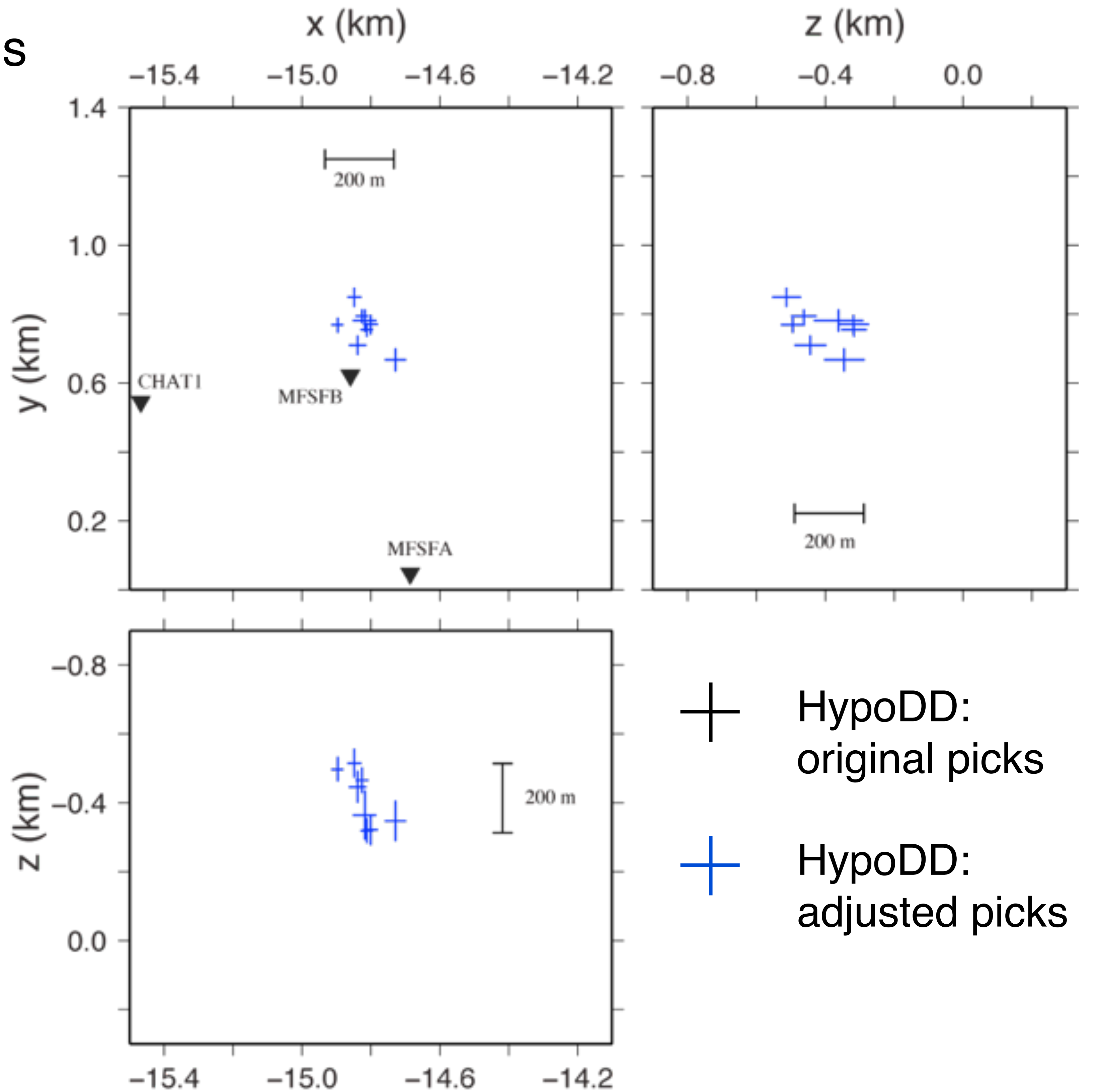

HypoDD relative relocations

Relative relocations still show some scatter
-> real or location artifact?

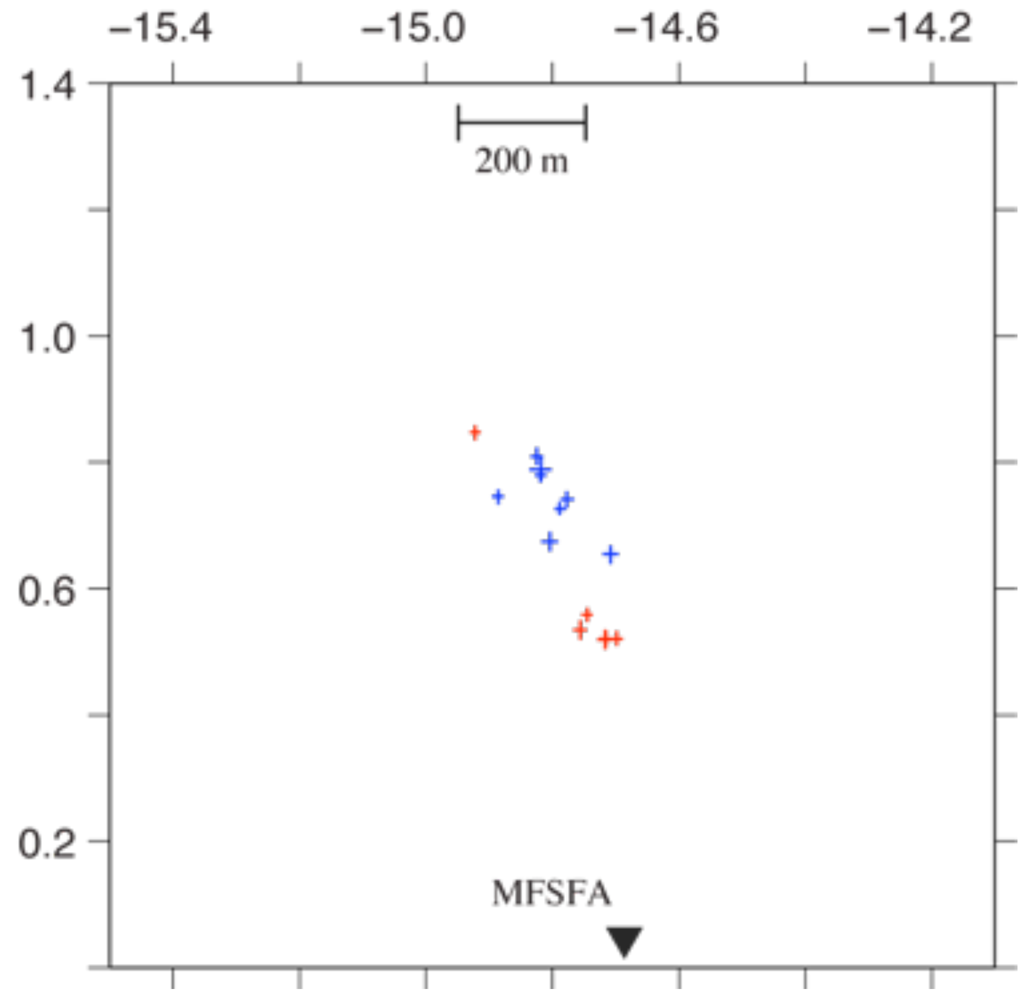

HypoDD relative relocations

Relative relocations still show
some scatter
-> real or location artifact?

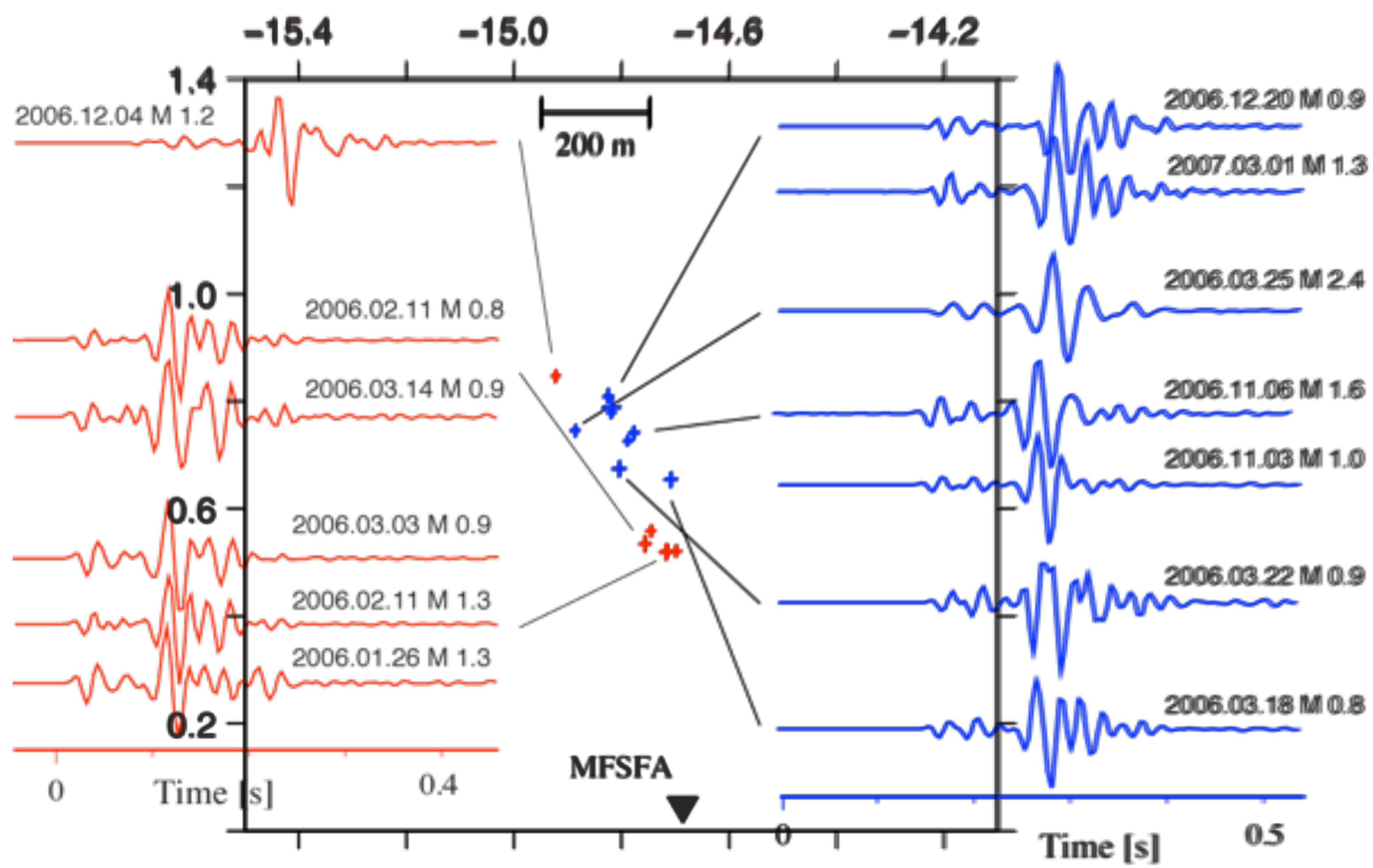

HypoDD relative relocations

Relative relocations still show some scatter
-> real or location artifact?

Location scatter is supported by waveform similarities.

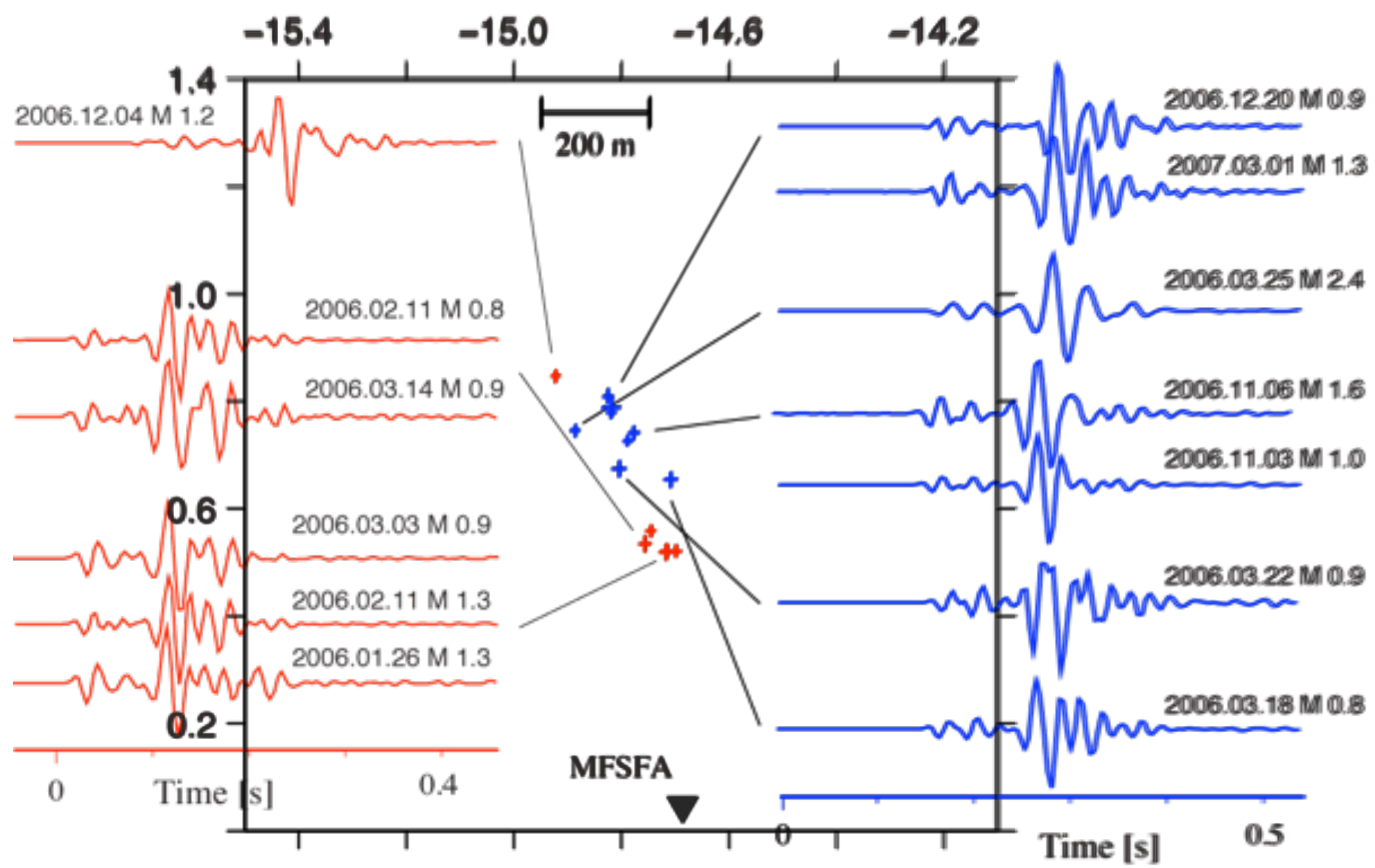

HypoDD relative relocations

Relative relocations still show some scatter
-> real or location artifact?

Location scatter is supported by waveform similarities.

Epicenter relocations show NW-SE alignment consistent with orientation of mapped faults zone and active fault plane of the M2.4 earthquake.

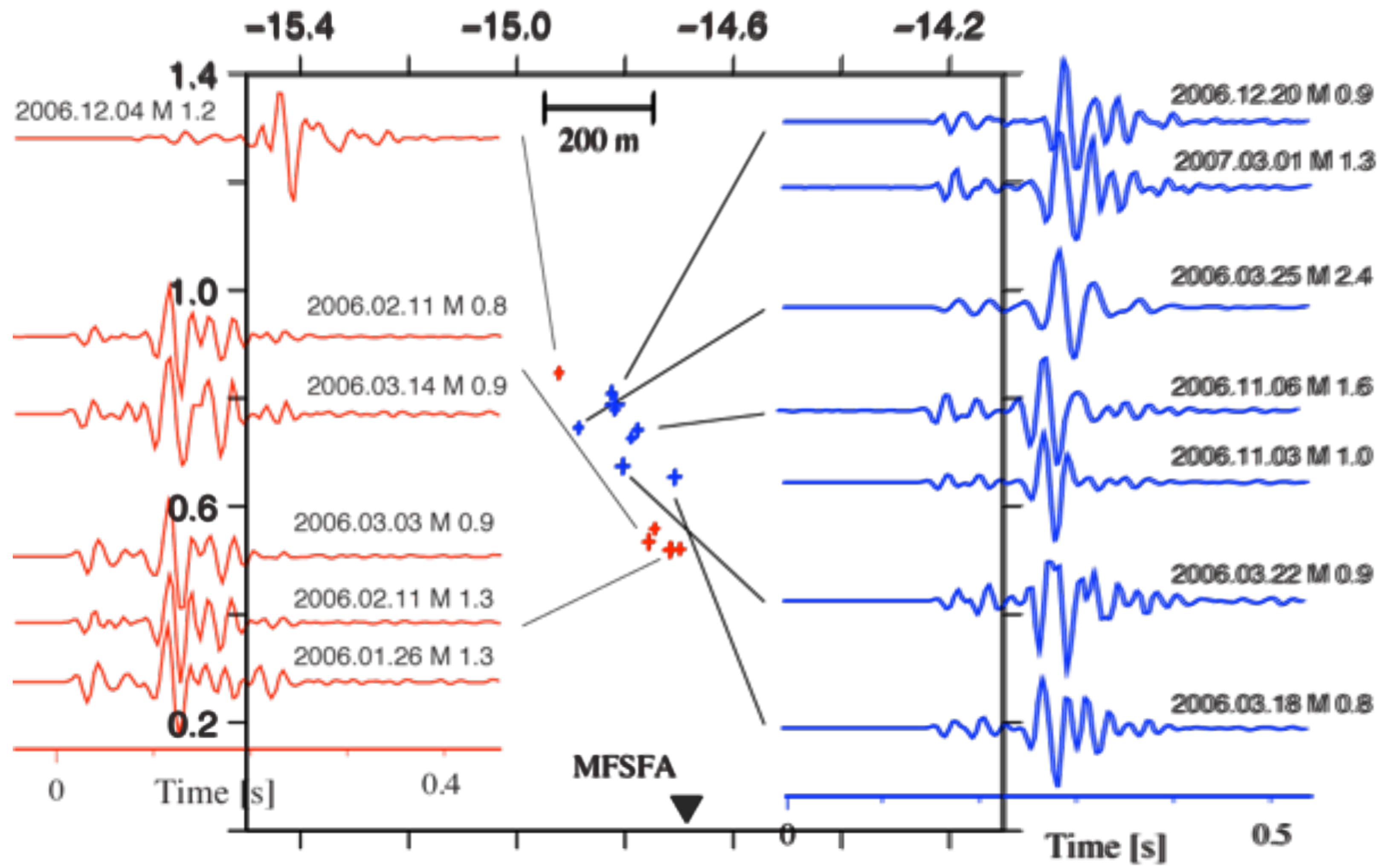

Source dimensions

Spectral inversion (Edwards et al., 2008) to compute Ω, f_c, $t^*+\kappa$

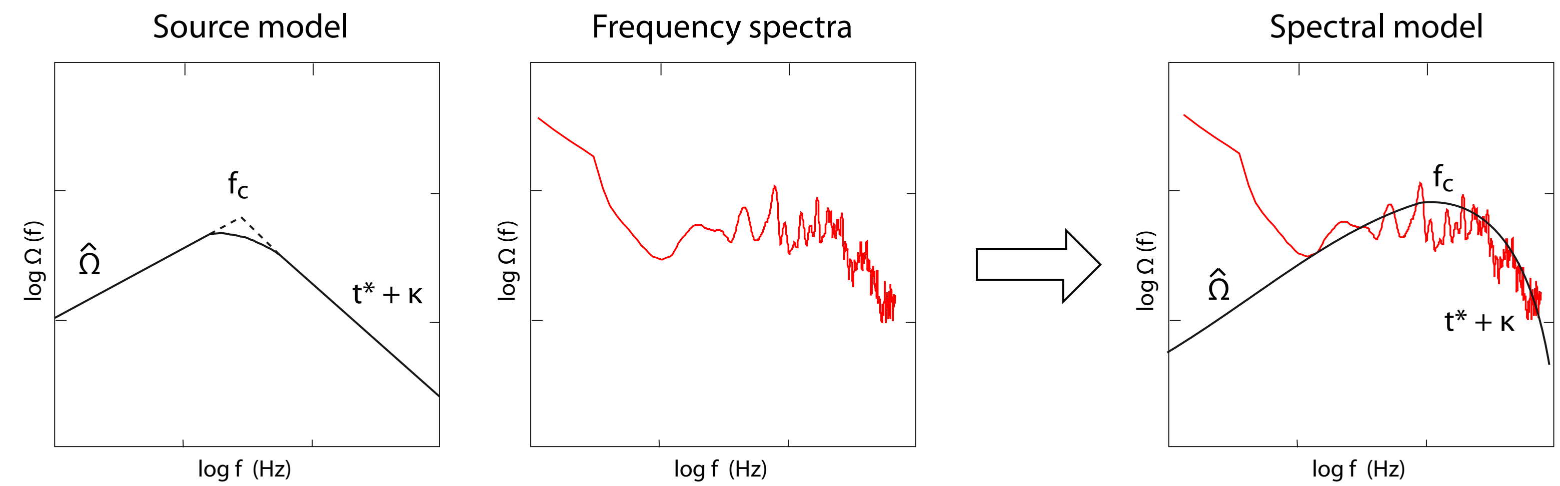

Use Madrigua's (1976) equation to relate f_c and source zone radius r_0:

$$r_0 = 1.32 \frac{v_s}{2\pi f_c}$$

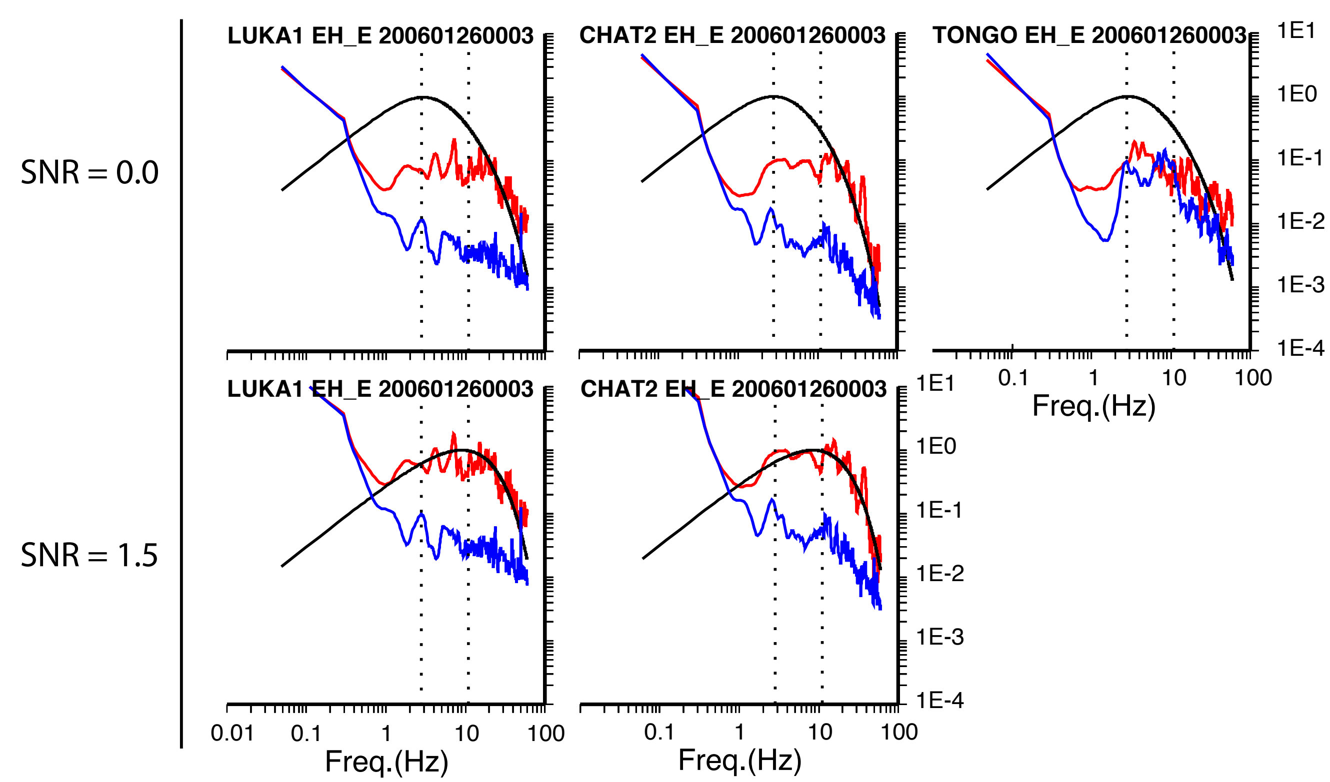

Signal-to-noise ratio (SNR) > 1.5 required -> in total 79 events could be processed.

Source dimensions

Source dimensions based on computed corner frequencies.

Each cluster represents an individual fault patch with overlapping rupture zones.

Each fault patch ruptured repeatedly during the seismic sequence.

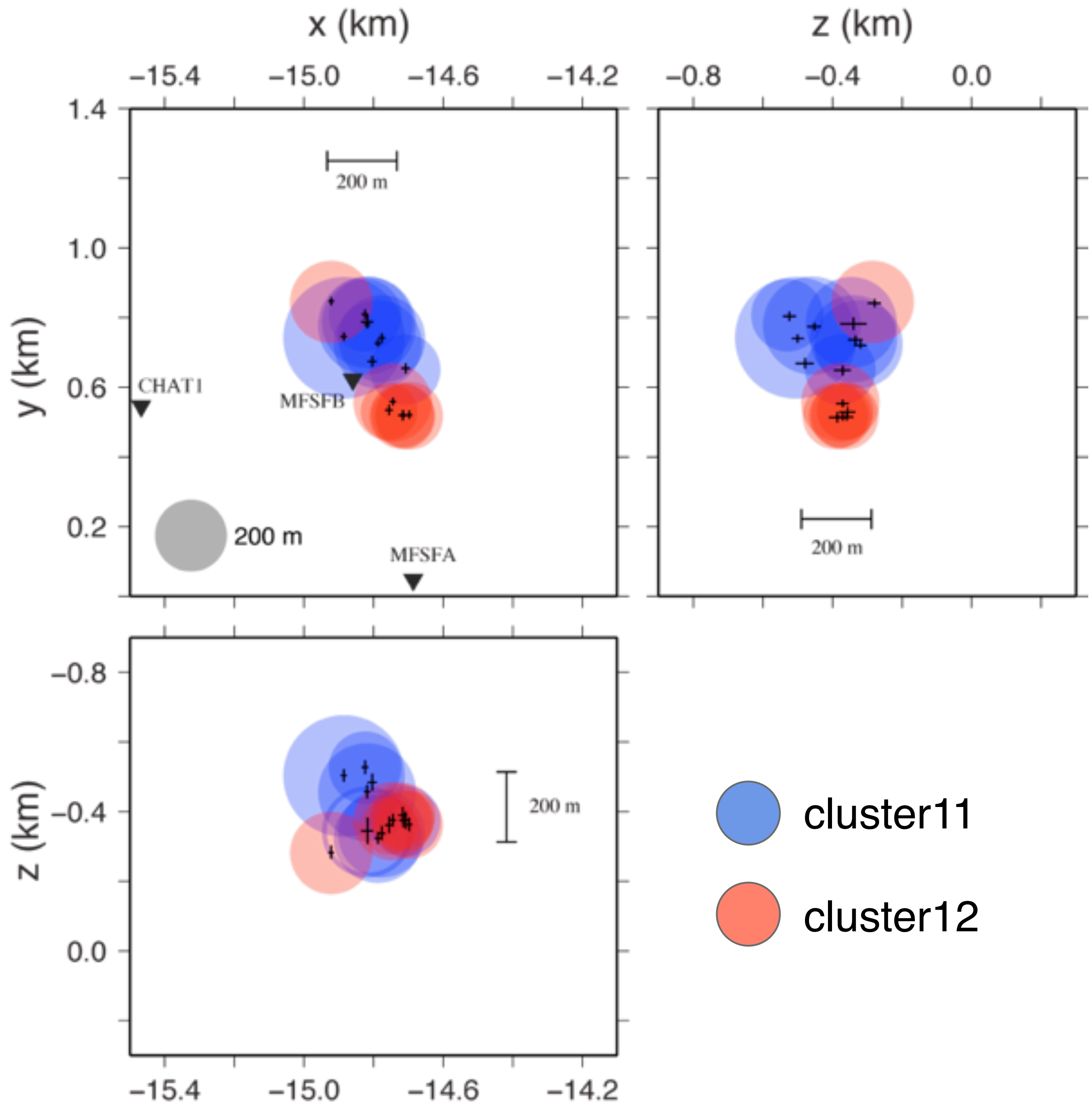

Summary of seismic observations

Earthquakes occurred mainly to the east of the fault zone in the brittle Lucomagno gneiss.

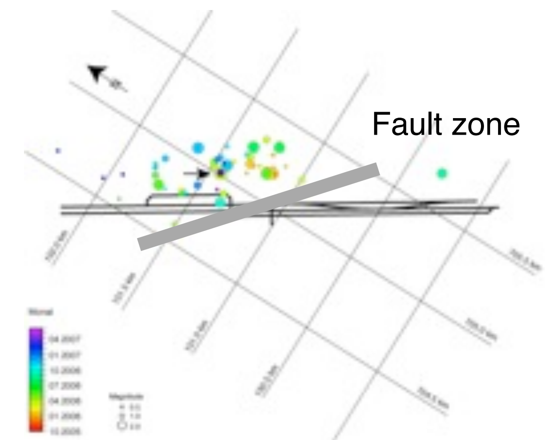

The largest earthquake (Ml=2.4) occurred likely on or along the fault zone.

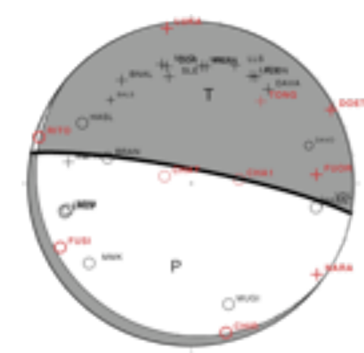

Several fault patches ruptured repeatedly.

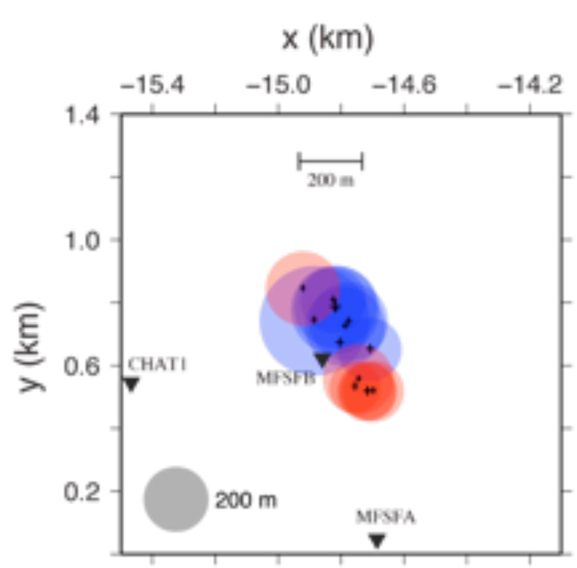

Fault model

Earthquakes occurred mainly on a complex system of steeply dipping faults.

Hypocenter locations and waveform similarity suggest that individual fault patches ruptured repeatedly.

These fault patches locate at 100 - 200 m distance from the tunnel and are parallel to the mapped fault zone.

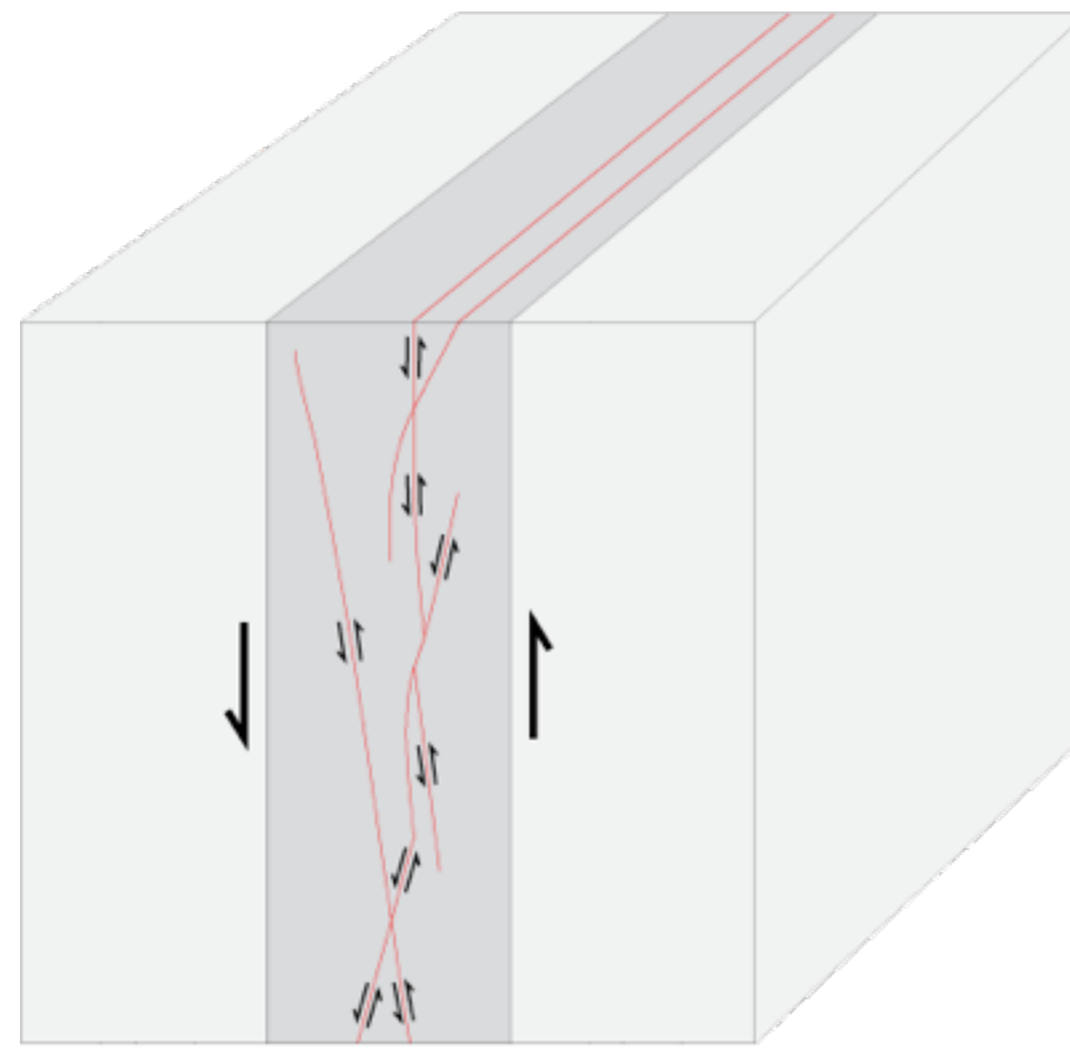

Distinct-element modeling of stress redistribution

Model set up

Two-dimensional modeling to assess static stress redistribution.

Material properties are taken from samples in the tunnel.

Initial stress conditions are given by load of the overburden (~30 MPa).

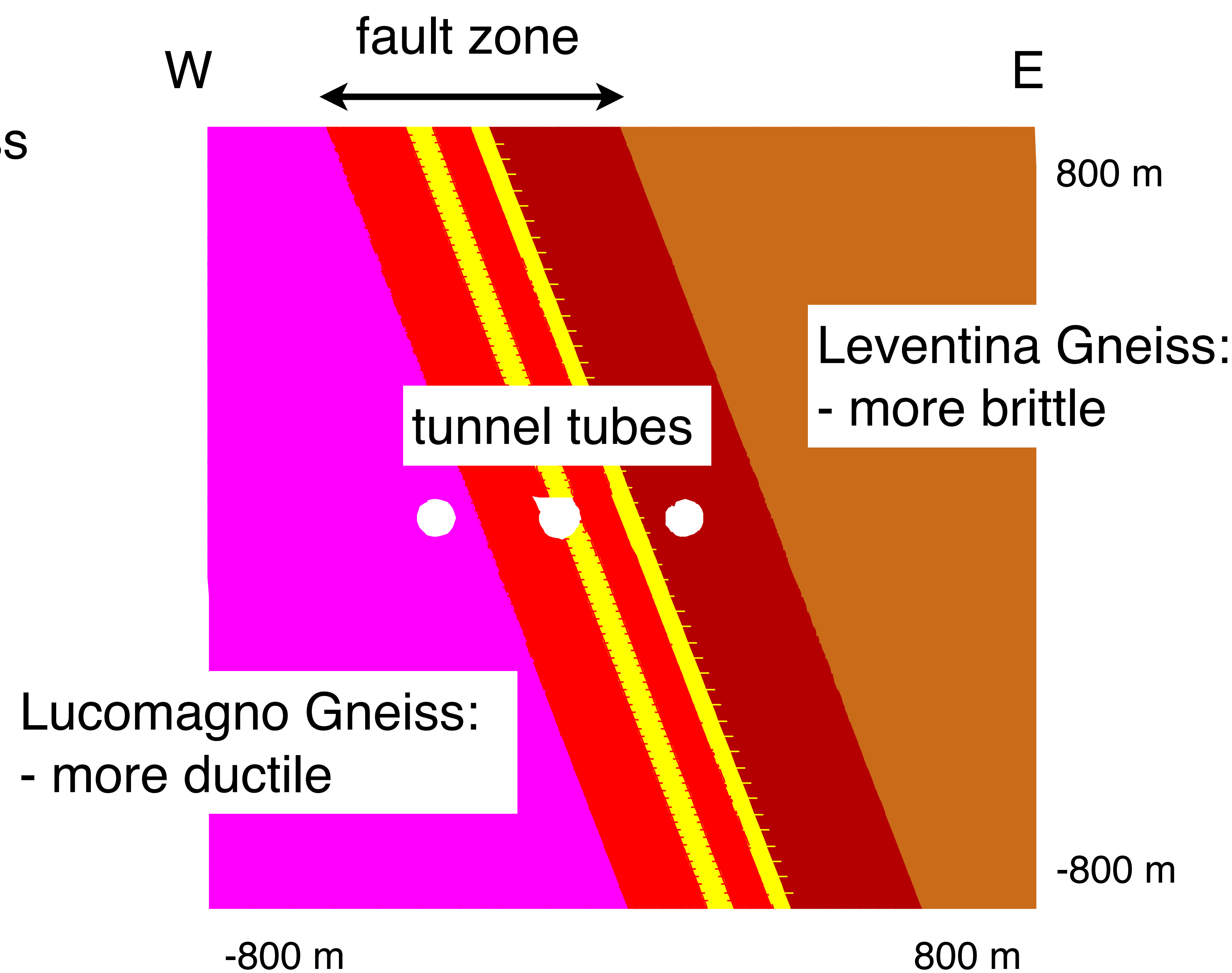

Distinct-element modeling of stress redistribution

Model set up

Two-dimensional modeling to assess static stress redistribution.

Material properties are taken from samples in the tunnel.

Initial stress conditions are given by load of the overburden (~30 MPa).

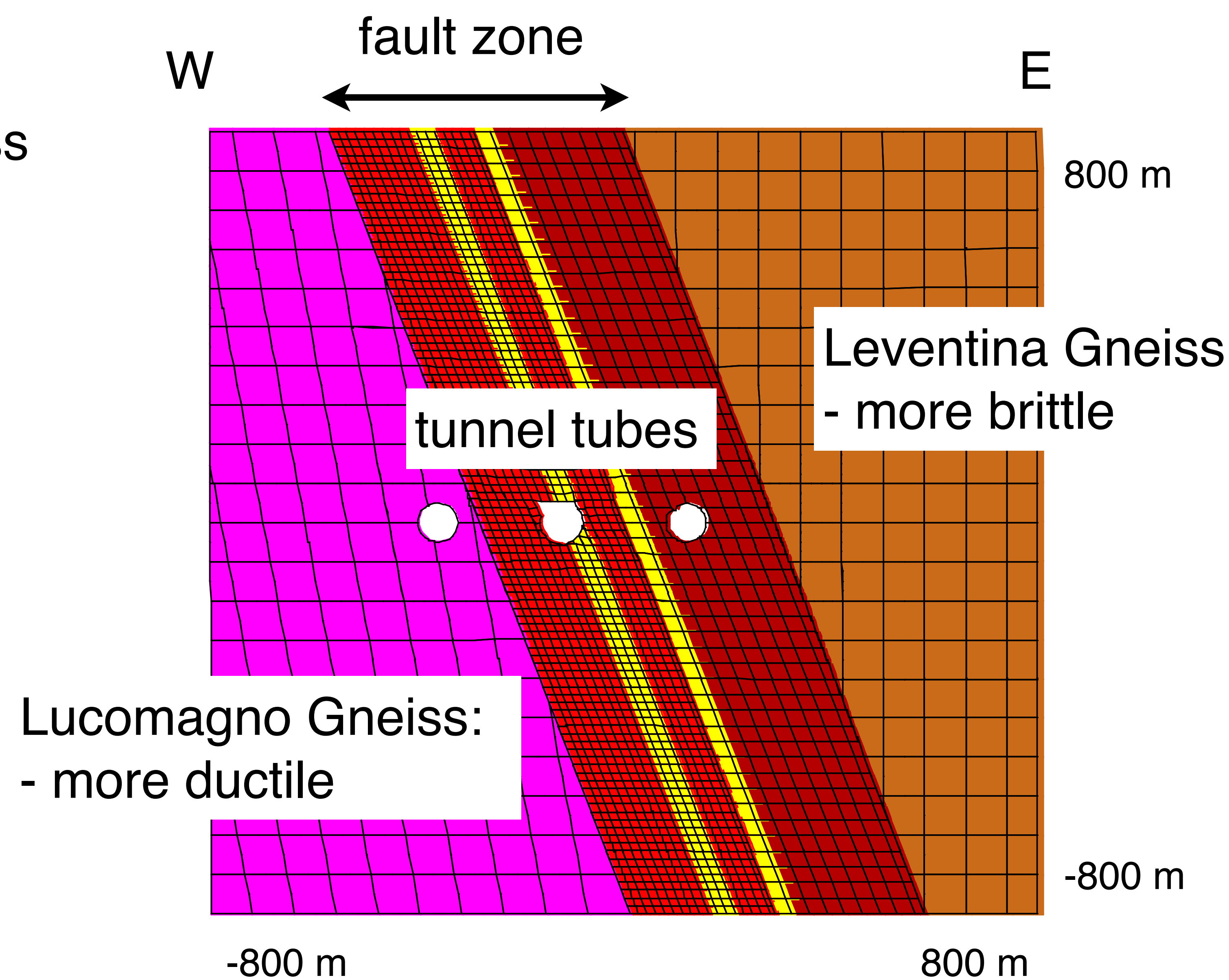

Distinct-element modeling of stress redistribution:

Vertical stresses

Strong decrease in vertical stresses (~20 MPa) around the tunnel tubes.

Large increase of vertical stresses (~30 MPa) to the East of the fault zone where earthquakes occurred.

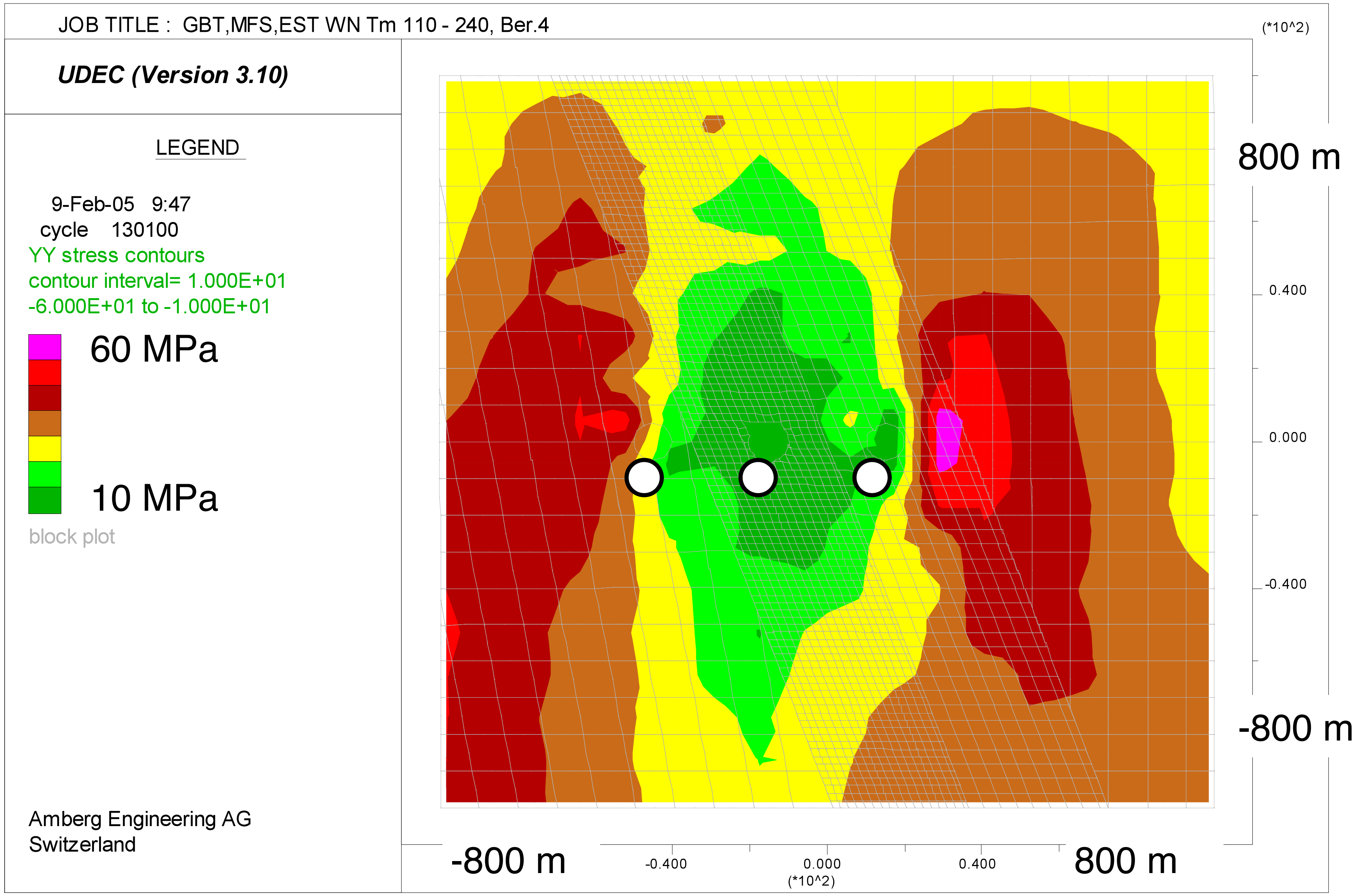

Distinct-element modeling of stress redistribution:

Vertical stresses

Strong decrease in vertical stresses (~20 MPa) around the tunnel tubes.

Large increase of vertical stresses (~30 MPa) to the East of the fault zone where earthquakes occurred.

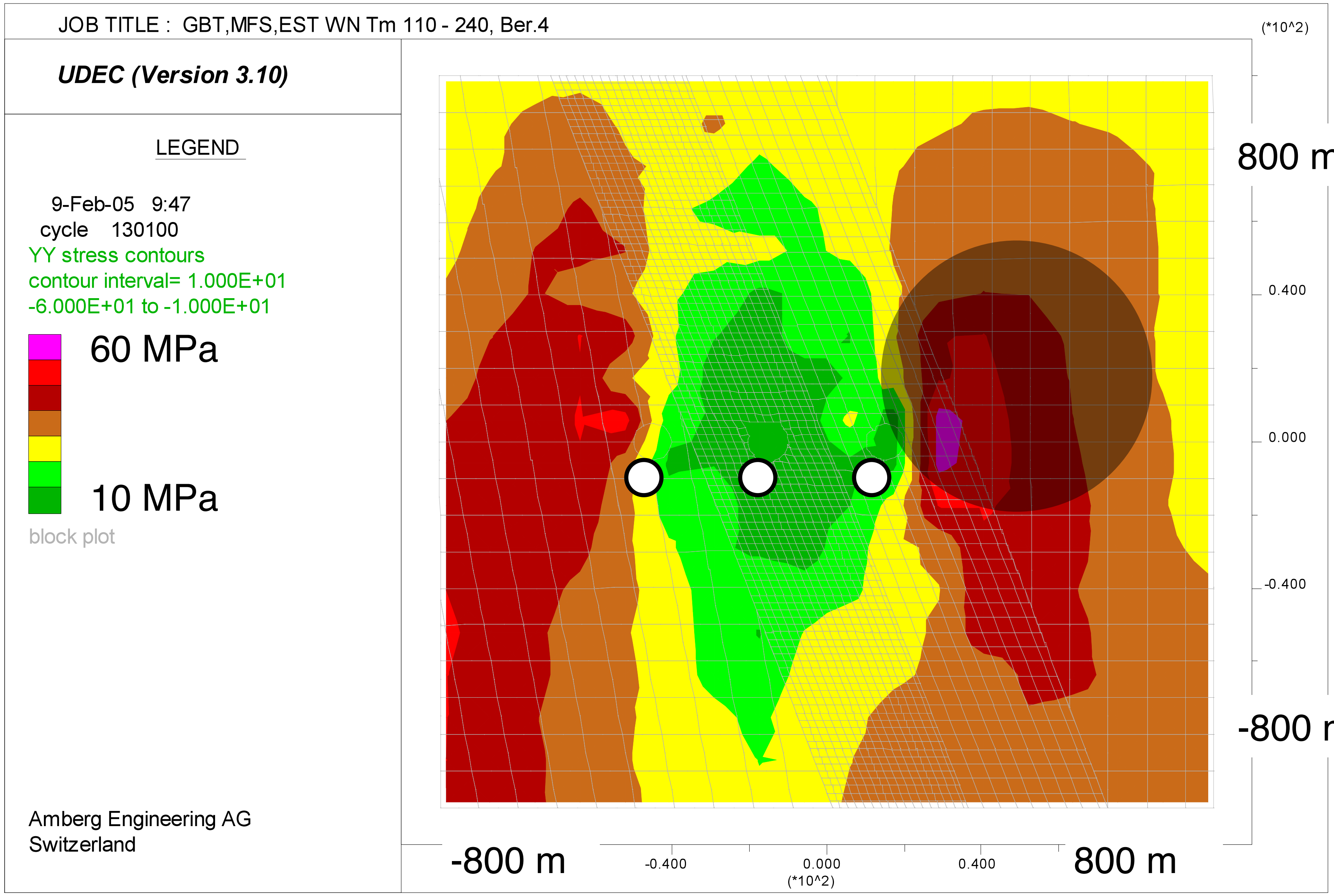

Possible mechanism for earthquakes in MFS Faido

Combination of excavation work and local geology lead to stress increase in the brittle Lucomango gneiss.

Photo: T. Eppler, Amberg Engineering

Possible mechanism for earthquakes in MFS Faido

Combination of excavation work and local geology lead to stress increase in the brittle Lucomango gneiss.

This stress increase in combination with existing stresses in the fault zone induced local failures (earthquakes).

Photo: T. Eppler, Amberg Engineering

Possible mechanism for earthquakes in MFS Faido

Combination of excavation work and local geology lead to stress increase in the brittle Lucomango gneiss.

This stress increase in combination with existing stresses in the fault zone induced local failures (earthquakes).

Ongoing excavation in combination with stress redistribution of previous earthquakes “re-charged” the system.

Photo: T. Eppler, Amberg Engineering

Possible mechanism for earthquakes in MFS Faido

Combination of excavation work and local geology lead to stress increase in the brittle Lucomango gneiss.

This stress increase in combination with existing stresses in the fault zone induced local failures (earthquakes).

Ongoing excavation in combination with stress redistribution of previous earthquakes “re-charged” the system.

With ceasing excavation activity a new stress equilibrium was established and seismicity stopped.

Photo: T. Eppler, Amberg Engineering

Conclusions

Be aware of systematic shifts in hypocenter locations due to improperly known velocity structure!

Conclusions

Be aware of systematic shifts in hypocenter locations due to improperly known velocity structure!

Earthquakes in the MFS Faido were likely induced by stress changes related to tunnel excavation.

Implications for seismic hazard and tunnel operation

Results indicate that stress redistribution did not occur over a larger region.

Implications for seismic hazard and tunnel operation

Results indicate that stress redistribution did not occur over a larger region.

Possibility for a larger (M>3) earthquake is therefore low.

Implications for seismic hazard and tunnel operation

Results indicate that stress redistribution did not occur over a larger region.

Possibility for a larger (M>3) earthquake is therefore low.

There remains a small risk that a small earthquake can occur very close to the tunnel with the potential of damage to tunnel wall.

Implications for seismic hazard and tunnel operation

Results indicate that stress redistribution did not occur over a larger region.

Possibility for a larger (M>3) earthquake is therefore low.

There remains a small risk that a small earthquake can occur very close to the tunnel with the potential of damage to tunnel wall.

Monitoring system during operation is recommended.

Thank You!